A Section 508–conformant HTML version of this article is available at https://doi.org/10.1289/EHP12758.

Evaluating the Effects of Chronic Oral Exposure to the Food Additive Silicon Dioxide on Oral Tolerance Induction and Food Sensitivities in Mice

Bruno Lamas,[1] Natalia Martins Breyner,[1]* Yann Malaisé,[1] Mark Wulczynski,[2] Heather J. Galipeau,[2] Eric Gaultier,[1] Christel Cartier,[1] Elena F. Verdu,[2]† and Eric Houdeau[1]†*

[1]Toxalim (Research Centre in Food Toxicology), Team Endocrinology and Toxicology of Intestinal Barrier, INRAE/ENVT/Paul Sabatier University, Toulouse, France
[2]Farncombe Family Digestive Health Research Institute, Department of Medicine, McMaster University, Hamilton, Ontario, Canada

Background: The increasing prevalence of food sensitivities has been attributed to changes in gut microenvironment; however, ubiquitous environmental triggers such as inorganic nanoparticles (NPs) used as food additives have not been thoroughly investigated.

Objectives: We explored the impact of the NP-structured food-grade silicon dioxide (*fg*-SiO_2) on intestinal immune response involved in oral tolerance (OT) induction and evaluated the consequences of oral chronic exposure to this food-additive using a mouse model of OT to ovalbumin (OVA) and on gluten immunopathology in mice expressing the celiac disease risk gene, HLA-DQ8.

Methods: Viability, proliferation, and cytokine production of mesenteric lymph node (MLN) cells were evaluated after exposure to *fg*-SiO_2. C57BL/6J mice and a mouse model of OT to OVA were orally exposed to *fg*-SiO_2 or vehicle for 60 d. Fecal lipocalin-2 (Lcn-2), anti-OVA IgG, cytokine production, and immune cell populations were analyzed. Nonobese diabetic (NOD) mice expressing HLA-DQ8 (NOD/DQ8), exposed to *fg*-SiO_2 or vehicle, were immunized with gluten and immunopathology was investigated.

Results: MLN cells exposed to *fg*-SiO_2 presented less proliferative T cells and lower secretion of interleukin 10 (IL-10) and transforming growth factor beta (TGF-β) by T regulatory and $CD45^+$ $CD11b^+$ $CD103^+$ cells compared to control, two factors mediating OT. Mice given *fg*-SiO_2 exhibited intestinal Lcn-2 level and interferon gamma (IFN-γ) secretion, showing inflammation and less production of IL-10 and TGF-β. These effects were also observed in OVA-tolerized mice exposed to *fg*-SiO_2, in addition to a breakdown of OT and a lower intestinal frequency of T cells. In NOD/DQ8 mice immunized with gluten, the villus-to-crypt ratio was decreased while the $CD3^+$ intraepithelial lymphocyte counts and the Th1 inflammatory response were aggravated after *fg*-SiO_2 treatment.

Discussion: Our results suggest that chronic oral exposure to *fg*-SiO_2 blocked oral tolerance induction to OVA, and worsened gluten-induced immunopathology in NOD/DQ8 mice. The results should prompt investigation on the link between SiO_2 exposure and food sensitivities in humans. https://doi.org/10.1289/EHP12758

Introduction

Adverse food reactions include food sensitivities, which are immune mediated, and food intolerance, which is the result of failure to digest the triggering agent, as in lactose intolerance.[1,2] Food sensitivities to protein antigens include allergic (e.g., peanut allergy) and autoimmune-mediated diseases, such as celiac disease, in which the main driver is gluten in wheat, rye, and barley.[2,3] Although distinct pathogenic mechanisms are involved in food sensitivities, failure to develop oral tolerance (OT) to the driver antigen is usually a common underlying mechanism.[4–6] Because the prevalence of food sensitivities continues to increase,[7,8] additional triggers and co-factors that promote breakdown of OT or a pro-inflammatory milieu, are suspected.[9–11] In this context, chronic exposure to inorganic nanoparticles (NPs) from various household sources, including their use as food additives, has gained increasing attention due to the potential immune system alterations that they can induce.[11,12] Notably, studies in rats[13] and mice[14,15] have demonstrated that silicon and titanium dioxide NPs can disrupt OT[14,15] or alter immune cell populations involved in OT induction,[13] respectively. Thus, foodborne NPs may be linked to the recent prevalence increase in food sensitivities in the industrialized world.

Food-grade silicon dioxide (*fg*-SiO_2) (INS 551), also known as synthetic amorphous silica (SAS), is one of the most widely used nanoparticular food additives worldwide, used as an anti-caking agent in powdered food (e.g., sugar, salt, milk, instant soups, and infant formula) among other texturing functions, such as viscosity control and emulsion stabilization.[16] These materials are nanostructured powders constituted of primary SiO_2 grains of ∼15–20 nm in diameter, aggregated together by covalent bonds or fused into dense and complex structure chaplets.[17,18] The use of *fg*-SiO_2 as a direct and indirect food ingredient has been concluded by the US Food and Drug Administration to be Generally Recognized as Safe at levels up to 2% in the finished food product. Based on average daily food consumption data from the 2015–2016 National Health and Nutrition Examination Survey, the mean and 90th percentile intake of *fg*-SiO_2 by the total US population aged 2 years and older were estimated as 46 and 103 mg/person/day, respectively.[19] In Europe, *fg*-SiO_2 is authorized *ad quantum satis* for technological purposes, and the European Food Safety Authority (EFSA) estimated that daily exposure ranges between 0.8 to 74.2 mg/kg of body weight (BW)/d in the general population, with infants (12 wk to 11 months old) being the highest exposed (i.e., 44 to 160 mg/kg BW/d in the 95th percentile).[16] Silicon (Si) has been detected in the ileum and colon mucosa following oral administration of SiO_2-NP models in mice,[20] and bioaccumulation of SiO_2 has been reported in Peyer's patches from human biopsies in adults[21] and children.[22] While short-term ingestion of nonfood sources of SiO_2-NPs induced low-grade intestinal inflammation[20] and impaired OT to ovalbumin (OVA) in male BALB/c

*These authors share co-first authorship.
†These authors share co-senior authorship.

Address correspondence to Bruno Lamas, INRAE Toxalim UMR 1331, 180 Chemin de Tournefeuille, 31027 TOULOUSE cedex 3, France. Email: bruno.lamas@inrae.fr. And, Eric Houdeau, INRAE Toxalim UMR 1331, 180 Chemin de Tournefeuille, 31027 TOULOUSE cedex 3, France. Email: eric.houdeau@inrae.fr

Supplemental Material is available online (https://doi.org/10.1289/EHP12758).

The authors declare they have nothing to disclose.

Conclusions and opinions are those of the individual authors and do not necessarily reflect the policies or views of EHP Publishing or the National Institute of Environmental Health Sciences.

Received 17 January 2023; Revised 8 January 2024; Accepted 17 January 2024; Published 21 February 2024.

Note to readers with disabilities: *EHP* strives to ensure that all journal content is accessible to all readers. However, some figures and Supplemental Material published in *EHP* articles may not conform to 508 standards due to the complexity of the information being presented. If you need assistance accessing journal content, please contact ehpsubmissions@niehs.nih.gov. Our staff will work with you to assess and meet your accessibility needs within 3 working days.

mice,[14] these studies employed supra-physiological doses in short periods of time, which are well above currently authorized food-grade doses of exposure. Thus, is it key to investigate chronic exposure to foodborne SiO_2 mimicking the manner in which they are consumed by the general population. This is timely, as although the role of environmental co-factors such as infections and alterations in the intestinal microbiota have been thoroughly studied,[23] the role of chronic ingestion of food additives composed of inorganic NPs is still largely unknown.

In the current study, we first assessed *in vivo* and *ex vivo* the impact of *fg*-SiO_2 exposure on the intestinal immune response involved in OT induction. Next, we used a mouse model of OT to OVA to determine whether chronic exposure to *fg*-SiO_2 at human-relevant levels, in solid or liquid matrix as dietary vehicles, blocks OT induction and induces gut inflammation. Finally, the role of chronic *fg*-SiO_2 administration on the development of food sensitivity with autoimmune pathophysiology was explored in a mouse model of gluten sensitivity expressing the celiac risk gene, HLA-DQ8.

Methods

Chemicals and Reagents

The SiO_2 sample was purchased as powder from a French commercial supplier producing food-grade (*fg*-SiO_2) precipitated amorphous silica (INS 551) in the frame of the PAIPITO project funded by the French National Research Agency.[17] For physicochemical characterization, *fg*-SiO_2 was sonicated (VCX 750-230V; Sonics and Materials, Inc.) in ultrapure water (1 mg/mL) for 1 min at 40% amplitude in an ice bath.[24] The hydrodynamic diameter (Z-average), polydispersity index, and zeta potential were determined using dynamic light scattering (DLS) (Zetasizer Nano ZS; Malvern Instruments Ltd.) with 10 µL of *fg*-SiO_2 suspension diluted in 2 mL of ultrapure water (Table S1).[24] Transmission electron microscopy (TEM) analysis was performed on a JEM 1400 (JEOL) equipped with camera Orius SC1000B (Gatan, Inc.) driven by DigitalMicrograph software (Gatan-Ametek). The sonicated suspension of *fg*-SiO_2 was diluted in ultrapure water (10 mg/mL), and size measurement was determined from bright-field TEM images by using the image processing open-source software ImageJ (NIH).

Ex Vivo *Exposure of MLN Cells to* fg-SiO_2 *and Flow Cytometry*

Six- to 7-wk-old male C57BL/6J mice were purchased from Janvier (France) and housed for 1 week in the INRAE Toxalim animal facility (temperature: 22 ± 2°C; relative humidity: 50 ± 20%; light/dark cycle: 12h/12h) with unlimited access to food (Mucedola 2018; Envigo) and water before being sacrificed to collect mesenteric lymph nodes (MLNs). Cell suspensions were immediately prepared from MLNs of these untreated mice (i.e., not exposed to *fg*-SiO_2) by pressing cells through a 70-µm cell strainer (BD Difco) in complete Dulbecco's modified Eagle medium (DMEM; Fisher Scientific) (10% heat-inactivated fetal calf serum, 2 mM L-glutamine, 50 IU/mL penicillin, and 50 µg/ml streptomycin; Sigma-Aldrich). Cells (1×10^6 cells/mL) were cultured (37°C, 10% CO_2) in 24-well plates (Costar; Corning) in the presence of (not dispersed) *fg*-SiO_2 (0, 6.25, 12.5, 25, and 50 µg/ml) and stimulated for 48 h with both phorbol 12-myristate 13-acetate (PMA) (50 ng/mL; Sigma-Aldrich) and ionomycin (1 µM; Sigma-Aldrich) ($n = 7$ per group for 0, 6.25, and 12.5 µg/mL, and $n = 8$ per group for 25 and 50 µg/mL) to activate all immune cells (nonspecific stimulation). For specific T cell stimulation, antibodies directed against CD3 (145-2C11; Invitrogen) and CD28 (37.51; Invitrogen) were diluted at 4 µg/mL in phosphate-buffered saline (PBS) and 0.5% bovine serum albumin (BSA) (500 µL/well) and incubated overnight at 4°C in 24-well plates (Costar; Corning). After washing with PBS, cell suspensions from MLN of untreated mice (1×10^6 cells/mL) were added to wells and exposed to *fg*-SiO_2 (0, 6.25, 12.5, 25, and 50 µg/mL) before incubation for 24 h at 37°C and 10% CO_2 ($n = 7$ per group for 0, 6.25, and 12.5 µg/mL and $n = 8$ per group for 25 and 50 µg/mL). Following centrifugation ($200 \times g$, 5 min at room temperature), the supernatants from cells stimulated with PMA and ionomycin or with CD3/CD28 antibodies were recovered and frozen at −80°C until processing. Enzyme-linked immunosorbent assays (ELISAs) were performed as described below in order to assess MLN cell production of interleukin 10 (IL-10), interferon gamma (IFN-γ), and transforming growth factor beta (TGF-β). For detection and phenotyping of cell subsets, MLN cell suspensions (5×10^5 cells/mL) were incubated (37°C, 10% CO_2) in 24-well plates (Costar; Corning) for 48 h with *fg*-SiO_2 (0, 6.25, 12.5, 25, and 50 µg/mL) before stimulation with PMA (50 ng/mL) and ionomycin (1 µM) for 5 h in presence of GolgiStop (0.67 µL/mL; BD Biosciences). These cells were harvested, washed, and incubated with CD16/CD32 Mouse Fc block (2.4G2; BD Pharmingen) in PBS supplemented with 3% fetal bovine serum for 20 min at 4°C. For surface staining, cells were washed and incubated with fluorescent-conjugated antibodies for 30 min at 4°C. The following antibodies were used at a final concentration of 1 µg/mL: CD3 (REA789; Miltenyi Biotec), CD4 (REA604; Miltenyi Biotec), CD25 (REA568; Miltenyi Biotec), CD45 (REA737; Miltenyi Biotec), CD103 (REA789; Miltenyi Biotec), and CD11b (REA592; Miltenyi Biotec). The intracellular staining was performed using a Cytofix/Cytoperm Kit Plus (BD Biosciences) according to the manufacturer's instructions and using the following antibodies at final concentration of 2 µg/mL: T-Bet (O4-46; BD Biosciences), IFN-γ (XMG1.2; BD Biosciences), FoxP3 (FJK-16s; eBioscience), IL-10 (JES5-16E3; BD Biosciences), and TGF-β (TW7-16B4; BD Biosciences). The data were collected using MACSQuant analyzer (Miltenyi Biotec) and were analyzed using FlowJo Software (Tree Star Inc.).

Cytotoxicity and Proliferation Assay in MLN Cells Exposed Ex Vivo *to* fg-SiO_2

MLN from untreated mice were sieved through a 70-µm cell strainer (BD Difco) in complete DMEM (10% heat inactivated fetal calf serum, 2 mM L-glutamine, 50 IU/mL penicillin, and 50 µg/ml streptomycin; Sigma-Aldrich). Viability was assessed by labeling cells with propidium iodide (PI) (Invitrogen). Cells (1×10^6 cells/mL) were cultured (37°C, 10% CO_2) in 24-well plates (Costar; Corning) in the presence of *fg*-SiO_2 (0, 6.25, 12.5, 25, and 50 µg/ml) for 48 h. After fixation with paraformaldehyde (4%; Sigma-Aldrich), cells were washed with PBS, centrifuged ($200 \times g$, 5 min at room temperature), and incubated at room temperature for 15 min with PI at 3 µM ($n = 4$ per group). The percentage of viability was measured by flow cytometry (MACSQuant analyser; Miltenyi Biotec). Data were analyzed using FlowJo Software (Tree Star Inc.) and normalized to control. To assess the effects of *fg*-SiO_2 on T cell proliferation, MLN cells from untreated mice were first incubated with CellTrace Violet (10 µM; Invitrogen) for 20 min at room temperature and washed with Cerrotini medium (Dulbecco modified Eagle medium supplemented with 8% heat-inactivated fetal calf serum, 36 mg/L asparagine, 116 mg/L arginine, 10 mg/L folic acid, 1 g/L 4-[2-hydroxyethyl]-1-piperazineethanesulfonic acid, 0.05 mmol/L β-mercapto-ethanol, 100 U/mL penicillin, 100 mg/mL streptomycin, and 1 µg/mL fungizone) for 5 min to remove the excess of the dye. Cells were then centrifuged at $200 \times g$ for 5 min at room temperature, seeded on 24-well plates (Costar; Corning) at 5×10^5 cells/mL in Cerrotini medium, and incubated with concanavalin-A (2 µg/mL; Sigma-

Aldrich) for 3 d with *fg*-SiO_2 (0, 6.25, 12.5, 25, and 50 μg/mL) ($n = 7$ per group). After centrifugation ($200 \times g$, 5 min at room temperature), cells were washed with CellWASH solution (BD biosciences) and labeled with Viobility 488/520 Fixable Dye (dilution 1:100; Miltenyi Biotec) for 15 min in the dark at room temperature to follow cell viability. After washing with PBS 0.5% BSA 2 mM EDTA and centrifugation ($200 \times g$, 5 min at room temperature), cells were labeled with antibodies directed against CD4 (1 μg/mL; REA604; Miltenyi Biotec) to identify T cells. The data were collected using MACSQuant analyzer (Miltenyi Biotec) and were analyzed using FlowJo Software (Tree Star Inc.).

Animals and fg-SiO_2 *Exposure*

Six- to 7-wk-old male C57BL/6J mice were purchased from Janvier (France) and housed in INRAE Toxalim animal facility. The animal room conditions were set as follows: temperature: 22 ± 2°C; relative humidity: 50 ± 20%; light/dark cycle: 12 h/12 h. All animal experiments were approved by the Local Animal Care and Use Committee (Comité d'Ethique pour l'Expérimentation Animale Toxalim Toulouse; TOXCOM 152-APAFIS#4746). For oral treatment with *fg*-SiO_2, the powder was extemporaneously suspended without preliminary dispersion protocol into sterile water for gastric gavage or incorporated into the food pellets in the INRAE animal feed preparation unit (SAAJ; Jouy-en-Josas, France) for exposure through a solid food matrix. The food pellets were replaced once a week throughout the experiments. As the adult human daily exposure levels to *fg*-SiO_2 estimated by EFSA ranges from 0.9 to 29.9 mg/kg BW/d depending on context,[16] mice were given *fg*-SiO_2 at 1 and 10 mg/kg BW/d for 60 d. A high dose of 100 mg/kg BW/d was also used to mimic *fg*-SiO_2 exposure levels in infants and children, which can reach 162.7 and 79.2 mg/kg BW/d, respectively, according to EFSA's worst-case scenario (i.e., last percentile of the maximum level scenario).[16] Mice were maintained in a pathogen-free environment and were randomly assigned (five, four, or three per cage) to three experimental series with unlimited access to food (Mucedola 2018; Envigo) and water.

In a first series of experiments, mice were fed with control diet (Mucedola 2018; Envigo) and gavaged (200 μL) daily for 60 d with *fg*-SiO_2 (1, 10, 100 mg/kg BW/d; $n = 8$ mice per group) or with the vehicle (sterile water; $n = 10$ mice) (see Figure 1A). Fresh stool samples from mice were collected before the sacrifice to determine fecal lipocalin-2 (Lcn-2) levels. At sacrifice, sections of ileum and colon were taken to assess intestinal permeability, and MLN were collected in order to evaluate the intestinal immune response by ELISA.

In the second series of experiments, mice were daily treated for 60 d with *fg*-SiO_2 (1, 10, 100 mg/kg BW/d) in sterile water suspension (gastric gavage; 200 μL) and assigned to OT protocol to OVA ($n = 7$ mice per group) (see Figure 3A). OT induction was assessed by measuring serum anti-OVA immunoglobulin G (IgG) at day 50, before the oral challenge with the same food antigen from day 55 to day 60. After collecting the feces, mice were sacrificed and the colon and MLN were removed. The colon was divided into two pieces, one (1 cm) for RNA extraction and the other (2 cm) to make explants, which, with the MLN, were used to assess the intestinal immune response.

In the last series of experiments, mice were exposed for 60 d to *fg*-SiO_2 (10 mg/kg BW/d) by gastric gavage (200 μL) or incorporated into food pellets (see Figure 4A). Control mice were gavaged with the vehicle (sterile water; 200 μL) and fed with control diet (Mucedola 2018; Envigo). Mice were first assigned to OT protocol to OVA ($n = 7$ per group) and serum anti-OVA IgG were determined at day 50, before being challenged with OVA from day 55 to day 60 by gastric gavage. The food intake per cage was measured twice a week and then divided by the number of mice per cage (3/4 mice per cage) and the number of days in order to estimate the food intake per mouse and per day. In mice exposed to the food additive through food pellets, the *fg*-SiO_2 exposure concentrations were calculated based on food intake and mice body weight measurement along the experiment (mean *fg*-SiO_2 dose of 8.58 ± 0.14 mg/kg BW/d). Before sacrificing the animals and collecting the MLN, fresh feces were collected. In some randomly chosen animals ($n = 5$ per group), the colon was also removed in order to extract RNA (1-cm piece) and isolate cells from the *lamina propria* (rest of the colon). In the three experimental series, all of the animals were sacrificed by cervical dislocation after 60 d of exposure to the food additive.

Measurement of Intestinal Permeability

Sections of ileum and colon were mounted in Ussing chambers (Easymount; Hamden) having a flux area of 0.5 cm^2 in order to evaluate the intestinal permeability as previously described.[25] Briefly, intestinal tissues were maintained at 37°C in oxygenated Krebs-Henseleit solution (Sigma-Aldrich). Mucosal-to-serosal transport of macromolecules was determined by adding fluorescein isothiocyanate (FITC)-labeled 4 kDa dextran (Sigma-Aldrich) in the luminal side of the chamber. After 1 h, fluorescence was measured in the serosal buffer with a fluorimeter (Tecan Spark), and the results were expressed as the flux of FITC dextran crossing 1 cm^2 of epithelium per hour ($nmol \cdot cm^{-2} \cdot h^{-1}$). Data are reported as the means of triplicate measurements.

Oral Tolerance to OVA

At day 41 of *fg*-SiO_2 exposure, ovalbumin (OVA; Sigma-Aldrich) (20 mg in 200 μL of PBS; OVA-tolerized mice) or PBS (Gibco; OVA-immunized mice; 200 μL) was administered once daily for 3 d by gastric gavage. At day 48, all mice were primed subcutaneously with 100 μg OVA in 100 μL of complete Freund adjuvant (CFA, InvivoGen) diluted in PBS (1:1 vol/vol). Blood was collected 6 d after and centrifuged at $10{,}000 \times g$ for 5 min at 20°C to recover the serum and to assess OT induction by measuring serum anti-OVA IgG levels. Then, all mice were gavaged with OVA (25 mg in 200 μL of PBS) once a day for 5 d (Table S2). Animals were sacrificed 1 h after the final OVA challenge by cervical dislocation. All OVA solutions were prepared extemporaneously throughout the experiment. Serum anti-OVA IgG levels were determined as described previously.[26] Briefly, OVA diluted at 25 μg/mL in PBS was incubated overnight in 96-well flat-bottomed plates. After washes with PBS and 0.05% Tween 20 (PBS-Tween), plates were incubated with PBS and 1% bovine serum albumin (Euromedex) to block nonspecific binding sites. Mice serum diluted at 1/10,000 in PBS was added to the wells after washes with PBS-Tween, and plates were then incubated overnight at 4°C. New washes with PBS-Tween were performed before incubating the plates at 37°C with a solution containing the horseradish peroxidase (HRP)-conjugated polyclonal goat anti-mouse IgG (HAF007; R&D system; dilution 1:2,500). The plates were washed with PBS-Tween, and tetramethylbenzidine (TMB) substrate (BioLegend) was added to each well before incubation at room temperature for 5 min. The reaction was stopped with 2 N H_2SO_4, and the absorbance of each well was read at 450 nm using a spectrometer (Tecan Spark).

Inflammation Markers

MLNs from each series of animal experiments above described were sieved through a 70-μm cell strainer (BD Difco) in complete DMEM (10% heat inactivated fetal calf serum, 2 mM L-glutamine, 50 IU/mL penicillin, and 50 μg/ml streptomycin; Sigma-Aldrich),

and 1×10^6 cells per well were cultured (37°C, 10% CO_2) in 24-well plates (Costar; Corning) for 48 h with stimulation by PMA (50 ng/mL; Sigma-Aldrich) and ionomycin (1 μM; Sigma-Aldrich). Following centrifugation ($200 \times g$, 5 min at room temperature), supernatants were recovered and frozen at −80°C until processing. To measure cytokine levels in the colonic explants, tissues from colon were isolated and rinsed in PBS. The colonic explants were cultured (37°C, 10% CO_2) overnight in complete DMEM in 24-well tissue culture plates (Costar; Corning). Supernatants were stored at −80°C until processing. ELISAs were performed according to the manufacturer's instructions: IL-10 (3432-1H-20; Mabtech) and IFN-γ (3321-1H-20; Mabtech) and TGF-β (DY1679; R&D system). For the colonic explants, cytokine concentrations were normalized according to the dry weight of each colonic explant.[27] Fecal Lcn-2 levels were determined as described previously.[28] Briefly, fresh stool samples from mice were collected before sacrifice, weighed, and stored at −80°C until processing. Fecal samples were suspended in cold PBS (100 mg/mL) and centrifuged for 5 min at $5{,}000 \times g$ and 4°C. Supernatants were collected and stored at −20°C until analysis. Lcn-2 levels in the supernatants were determined using the murine Lcn-2 ELISA kit (DY1857; R&D system) according to the manufacturer instructions.

Lamina Propria *Cell Isolation and Flow Cytometry*

After removing 1 cm of colon for RNA extraction, *lamina propria* cells were isolated from the rest of the colon as previously described.[27] Briefly, colon were placed in ice-cold Hank's balanced salt solution and opened longitudinally after removal of residual fat tissue. Colon were cut into 1-cm pieces, and after washes in ice-cold Hank's balanced salt solution, tissues were incubated twice in 20 mL of serum-free media with 5 mmol/L EDTA and 0.145 mg/mL dithiothreitol at 37°C and 250 rpm for 20 min. After each incubation, the colon pieces were washed with serum-free media containing 2 mmol/L EDTA, and the epithelial cell layer was removed by intensive vortexing and passing through a 40-μm cell strainer. Colon pieces were next digested in serum-free media containing Liberase (Roche Applied Science) and DNase I at 37°C and 250 rpm for 30 min. Cells were washed and resuspended in 4.5 mL of 44% Percoll and placed on 2.3 mL of 67% Percoll before centrifugation for 20 min at $600 \times g$ at room temperature. Cells were collected at the interphase of the Percoll gradient and washed in PBS supplemented with 3% of fetal bovine serum. Cells were then stained as previously described.[27] Briefly, after incubation with CD16/CD32 Mouse Fc block (2.4G2; BD Pharmingen) in PBS supplemented with 3% of fetal bovine serum for 20 min at 4°C, cells were washed and stained with fluorescent-conjugated antibodies for 20 min at 4°C. The cell phenotypes were analyzed with antibodies directed against CD45 (REA737; Miltenyi Biotec), CD11b (REA592; Miltenyi Biotec), and CD103 (REA789; Miltenyi Biotec) to identify subsets of antigen-presenting cells including subpopulations of dendritic cells (DC) and macrophages; CD3 (REA641; Miltenyi Biotec), CD4 (REA604; Miltenyi Biotec), and CD25 (REA568; Miltenyi Biotec) were used to identify T cells. Cell viability was assessed using Viobility 405/452 Fixable Dye (Miltenyi Biotec). All antibodies were used at final concentration of 1 μg/mL. The data were collected using MACSQuant analyzer (Miltenyi Biotec) and were analyzed using FlowJo Software (Tree Star Inc.).

Gene Expression Analysis Using Quantitative Reverse Transcription PCR (qRT-PCR)

Total RNA was isolated from colon samples using RNeasy Mini Kit (Qiagen). Quantitative RT-PCR was performed using iScript Reverse Transcriptase (Bio-Rad) and then a Takyon SYBR Green PCR kit (Eurogentec) in an ABI 7300 apparatus (Applied Biosystems) with specific mouse oligonucleotides (Eurogentec) described in Table S3. Thermal cycle conditions were 10 min at 95°C, then 40 cycles of 15 s at 94°C, 45 s at 58°C, and 30 s at 72°C followed by 5 min at 72°C. We used the $2^{-\Delta\Delta Ct}$ quantification method with mouse *Rpl19* as an endogenous control and the OVA-tolerized mice not exposed to *fg*-SiO_2 or nonobese diabetic (NOD) mice expressing HLA-DQ8 (NOD/DQ8) not exposed to *fg*-SiO_2 group as calibrator.

Gluten Sensitization and Challenge

For the gluten sensitivity model, experiments were performed in specific pathogen-free (SPF) NOD AB° DQ8 (NOD/DQ8) mice bred and housed in McMaster's Central Animal facility. Original breeding pairs were obtained from Mayo Clinic (USA, provided by Professor Joseph Murray). Protocols were approved by the Canadian and McMaster's Research Ethics Board for animal experimentation. As oestrogen production can modulate intestinal inflammation, only male mice were used in this experiment to reduce potential heterogeneity in the results. Male 8- to 12-wk-old SPF NOD/DQ8 mice were maintained on a gluten-free diet (Envigo; TD.05620) until gluten sensitization.[29] All mice had unlimited access to food and water. Mice were gavaged daily (200 μL) with the vehicle (sterile water) or the *fg*-SiO_2 (10 mg/kg BW/d) for 75 d. At day 40 after the beginning of *fg*-SiO_2 exposure, mice were sensitized with 500 μg of pepsin-trypsin digest of gliadin and 25 μg of cholera toxin (Sigma-Aldrich) by oral gavage (200 μL) once a week for 3 wk, to break OT to gluten.[29–31] Gluten-sensitized mice were then challenged orally (200 μL) with 10 mg of gluten (Sigma-Aldrich) dissolved in acetic acid three times a week for 2 wk (see Figure 5A) and referred to as gluten-treated mice.[29–31] Mice were sacrificed by cervical dislocation 6 d after the last sensitization (day 60; $n = 5$ mice per group) and 18 to 24 h after the final gluten challenge (day 75; $n = 6$ mice per group).

Assessment of Gluten-Immunopathology

Cross sections of the proximal small intestine were fixed in 10% formalin, embedded in paraffin, and cut to 4-μm sections for imaging with brightfield microscopy (Olympus). After sections were stained with hematoxylin and eosin, twenty villi and adjacent crypts were measured and ratioed in a blinded fashion from three intestinal sections taken 4 mm apart for each mouse using QuPath software. The presence of $CD3^+$ intraepithelial lymphocytes (IELs) was assessed using immunohistochemical staining using the same sections of the proximal small intestine. In brief, the sections were deparaffinized with xylenes, and endogenous peroxidase activity was blocked by incubation with dual endogenous enzyme blocking solution for 10 min (S200389-2; Agilent) before antigen retrieval using proteinase K incubation for 10 min. Nonspecific binding was blocked by 2 h incubation with 1% BSA in PBS. The primary antibody was incubated overnight at 4°C (1:1,000 polyclonal rabbit antihuman CD3; A045229-2; Agilent) and washed with PBS-Tween before incubation with HRP-conjugated secondary antibody for 30 min (EnVision+ system, K400311-2; Agilent). The IELs were visualized by incubating with 3,3′-diaminobenzidine (DAB+ substrate chromagen system, K346811-2; Agilent) followed by counterstaining with 60 s of Mayer's hematoxylin (S330930-2; Agilent). IELs were quantified by counting $CD3^+$ cells per 20 enterocytes in five randomly chosen villus tips using QuPath.

Anti-gliadin and anti-transglutaminase 2 (tG2) IgG2c were measured in serum by direct ELISA. A 96-well plate was coated with either transglutaminase (0.1 μg/well; T5398-2UN; Sigma-

Aldrich) diluted in PBS or gliadin (5 μg/well; G3375; Sigma-Aldrich) dissolved in 70% ethanol and diluted in PBS. Nonspecific binding was blocked with 2% BSA in PBS-Tween before 50 μL of serum was added to the wells for 2 h. After washes with PBS-Tween, HRP-conjugated secondary anti-mouse IgG2c (1:5,000; Sigma-Aldrich) antibodies were added to the wells for 1 h at room temperature. The plates were washed with PBS-Tween, and TMB substrate (Agilent) was added to each well before incubation at room temperature for 5 min. The reaction was stopped with 2 N H_2SO_4, and the absorbance of each well was read at 450 nm using a SpectraMax M3 plate reader (Molecular Devices).

Statistical Analysis

GraphPad Prism version 6.0 was used for all analyses. Data are presented as median (interquartile range) ± standard error of the mean (SEM). Normal distribution was determined by Kolmogorov-Smirnov test. For datasets that failed normality tests, nonparametric tests were used. Multiple comparisons were evaluated statistically by one-way analysis of variance (ANOVA) and post hoc Tukey test or nonparametric Kruskal-Wallis test followed by a post hoc Dunn's test. For comparisons between two groups, significance was determined using the two-tailed Student's *t*-test or nonparametric Mann-Whitney test. Numbers and tests used are provided in each figure legend. Differences corresponding to $P < 0.05$ were considered significant. Animals were randomly assigned to experimental groups. All analyses were performed unblinded and were adjusted for multiple comparisons. Sample size was estimated according to previous experience using the models described. No statistical method was used to predetermine sample size.

Results

Physicochemical Characterization of Food-Grade SiO_2 Particles

Consistent with previous physicochemical data of the commercial batch of silicon used in the current study, the *fg*-SiO_2 powder in water suspension formed large agglomerates of fused SiO_2-NPs of which the primary diameters ranged between 15 and 20 nm (Figure S1). In the current preparations, the mean hydrodynamic diameter of the agglomerates was 2,406 nm and polydispersity index was 0.20 (Table S1). As expected, the formation of large agglomerates was confirmed by a negative zeta potential (−25 mV) (Table S1).

Fecal Lipocalin-2, Gut Permeability, and Pro- and Anti-Inflammatory Cytokine Levels in Food-Grade SiO_2-exposed Mice

We first studied the impact of oral chronic exposure to *fg*-SiO_2 on intestinal immune response (Figure 1A). Fecal Lcn-2 protein level, a noninvasive marker of gut inflammation,[32] as well as pro- and anti-inflammatory cytokines and intestinal permeability were determined. Compared to control mice, fecal Lcn-2 was higher in mice exposed to *fg*-SiO_2 at any dose, with a peak at 10 mg/kg BW/d (Figure 1B). Increased production of the pro-inflammatory cytokine IFN-γ by MLN cells was observed in all mice exposed to *fg*-SiO_2, but the increase was only significant in mice exposed to 10 mg/kg BW/d of *fg*-SiO_2 compared with controls (Figure 1C). MLN cells from mice exposed to *fg*-SiO_2 showed lower production of the anti-inflammatory cytokines IL-10 and TGF-β compared with controls not exposed to the food additive (Figure 1D,E). No differences in ileal and colonic permeability were observed between control and *fg*-SiO_2-exposed mice (Figure S2).

Viability, Proliferation, and Cytokine Production of MLN Cells after Ex Vivo *Exposure to* fg-SiO_2

To determine whether the *fg*-SiO_2-mediated immunological defects could result from a direct interaction of SiO_2 particles with immune cells, MLN cells from untreated mice were exposed *ex vivo* to the food additive. Cell viability was analyzed by flow cytometry using propidium iodide. Results showed that MLN cell viability was not impacted after exposure to *fg*-SiO_2 regardless of the dose tested (Figure S3A). MLN cells were then stimulated in the presence of different doses of *fg*-SiO_2 using an unspecific simulation with PMA and ionomycin or an anti-CD3/CD28 stimulation specific of T cells, and the production of TGF-β, IL-10, and IFN-γ was assessed in the supernatant. Less TGF-β was observed in anti-CD3/CD28–stimulated cells after exposure to the highest dose of *fg*-SiO_2 while TGF-β secretion was not altered in PMA and ionomycin stimulation (Figure 2A,B). In the presence of *fg*-SiO_2, the production of the anti-inflammatory cytokine IL-10 was lower, regardless of MLN cell stimulation, but the decrease was only significant in PMA- and ionomycin-stimulated cells exposed at the highest doses of the food additive (Figure 2C,D). The production of IFN-γ by MLN cells was not different in the presence of *fg*-SiO_2 regardless of the stimulation used (Figure 2E, F). Flow cytometry analysis showed lower intracellular TGF-β in $CD45^+$ $CD103^+$ $CD11b^+$ cells [which includes dendritic cell (DC) and macrophage subpopulations] and lower production of IL-10 by regulatory T (Treg) cells ($CD3^+$ $CD4^+$ $CD25^+$ $FOXP3^+$ $IL\text{-}10^+$) after exposure to *fg*-SiO_2 (Figure 2G–I; Figures S3B–F, S4, and S5). In proliferative condition (i.e., coculture with concanavalin-A), MLN cells exposed to *fg*-SiO_2 had lower T cell proliferation (Figure 2J; Figure S6), which was similar in T cell viability compared with control (Figure S3G).

Oral Tolerance Induction to OVA and Intestinal Cytokine Production after OVA Oral Challenge in Food-Grade SiO_2-exposed Mice

We then explore whether the immunomodulatory effects of *fg*-SiO_2 could disrupt OT *in vivo*. Mice were exposed to different doses of the food additive and then given the food antigen model ovalbumin (OVA) by oral gavage (or PBS as control) to induce OT before subsequent immunization with the same antigen (Figure 3A). Anti-OVA IgG antibodies were first measured in sera collected on day 50 to assess OT induction in *fg*-SiO_2-treated mice (Figure 3A). In the absence of *fg*-SiO_2 treatment, OVA-tolerized mice exhibited lower OVA-specific IgG secretion compared to immunized mice (PBS), demonstrating OT induction (Figure 3B). In contrast, distinctly higher levels of anti-OVA IgG were observed in all OVA-tolerized mice with *fg*-SiO_2 treatment compared with OVA-tolerized mice not exposed to the food additive (Figure 3B).

We then evaluated the intestinal immune response in OVA-tolerized mice orally treated with the *fg*-SiO_2 after a *de novo* oral challenge to OVA (D60) to assess whether OT failure following exposure to the food additive may lead to food hypersensitivity (Figure 3A). Foodborne SiO_2-treated mice with oral OVA challenge had higher levels of fecal Lcn-2, *Il1β* expression in the colon, and IFN-γ production in MLN when compared with OVA-tolerized controls; these differences appeared to be dose-dependent and suggested gut inflammation (Figure 3C–E). IFN-γ was significantly higher at 10 mg/kg BW/d of *fg*-SiO_2 only (Figure 3E). In the same group of mice, we found lower expression of *Il10* and *Tgfβ* at all doses (Figure 3F,G). The IL-10 and TGF-β impairment in *fg*-SiO_2-treated OVA-tolerized mice was confirmed at protein level in MLN cells and in the colon for TGF-β (Figure 3H–J).

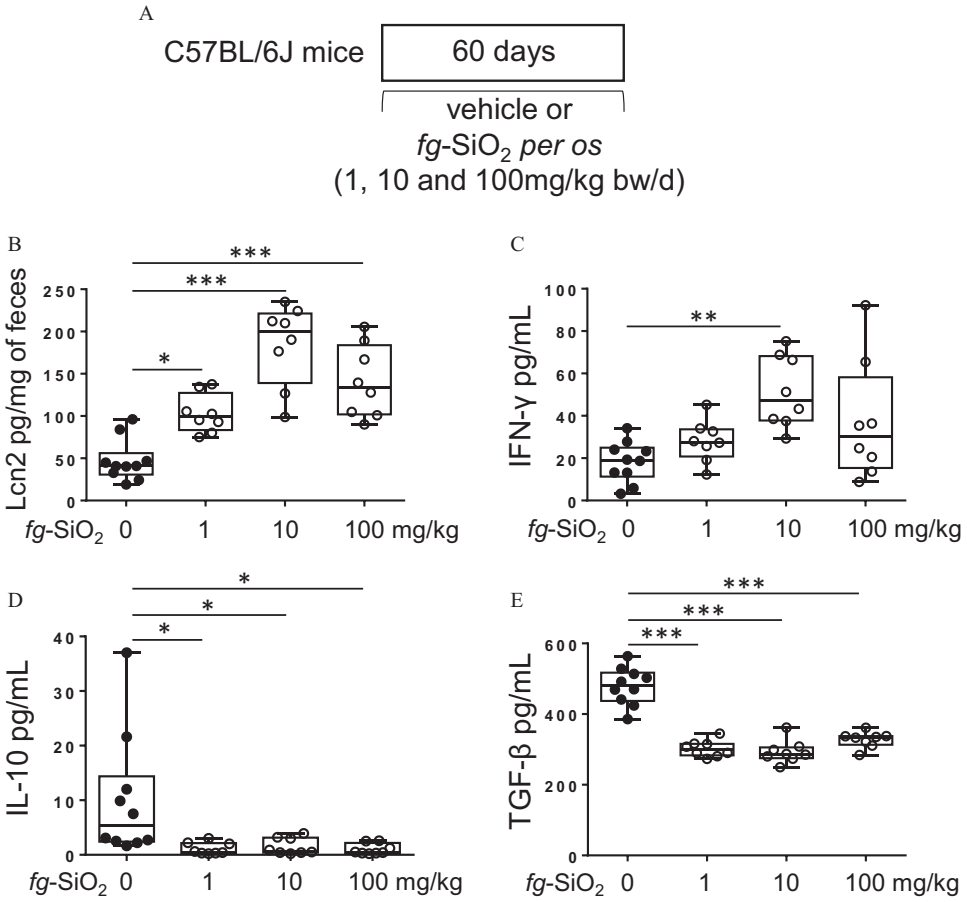

Figure 1. Intestinal immune response in mice after oral exposure to food-grade SiO_2. (A) The protocol for testing the effects on intestinal immune response of daily exposure of C57BL/6J mice to the vehicle (water) or to the food-grade SiO_2 (*fg*-SiO_2; 1, 10, or 100 mg/kg BW/d) through gavage. (B) Fecal lipocalin-2 (Lcn2) levels in mice orally exposed to food-grade SiO_2 (*fg*-SiO_2) ($n = 8$ mice per group) or to the vehicle ($n = 10$) for 60 d. (C–E) Amounts of IFN-γ (C), IL-10 (D), and TGF-β (E) secreted by mesenteric lymph node cells from mice orally exposed to *fg*-SiO_2 ($n = 8$ mice per group) or to the vehicle ($n = 10$) for 60 d. The data are expressed as median with interquartile range and whiskers extending from minimum to maximum ± SEM. $^{*}p < 0.05$; $^{**}p < 0.01$; $^{***}p < 0.001$ by one-way ANOVA and post hoc Tukey test. Data behind graphs are reported in Table S4. Note: ANOVA, analysis of variance; BW, body weight; IFN-γ, interferon gamma; IL-10, interleukin 10; SEM, standard error of the mean; TGF-β, transforming growth factor beta.

Frequency of Intestinal T Cells Involved in OT Induction after Chronic Exposure to fg-*SiO_2 through Either Gastric Gavage or Food Pellets*

To evaluate the impact of food matrices on the immunomodulatory effects of *fg*-SiO_2, mice were exposed to *fg*-SiO_2 in water suspension or incorporated into food pellets at 10 mg/kg BW/d and then OT to OVA was induced (Figure 4A). OVA tolerance protocol in mice not treated with *fg*-SiO_2 resulted in significantly lower circulating anti-OVA IgG levels compared with that of the oral PBS group, showing normal OT induction to OVA (Figure 4B). In contrast, anti-OVA IgG remained high in all OVA-tolerized mice exposed to *fg*-SiO_2, supporting failure of OT to OVA, regardless of the *fg*-SiO_2 vehicle (Figure 4B).

When focusing on OVA-tolerized mice exposed to *fg*-SiO_2 through food pellets, *de novo* oral challenge with OVA led to gut inflammation as shown by higher fecal Lcn-2 levels, higher IFN-γ production by MLN cells, and lower IL-10 and TGF-β levels as compared with OVA-tolerized controls (Figure 4A,C–F). These results showed that intestinal inflammation after restimulation by oral OVA in mice exposed to *fg*-SiO_2 was independent of food matrix.

We next evaluated frequency of $CD45^+$ $CD11b^+$ $CD103^+$ cells and of $CD3^+$ $CD4^+$ $CD25^{+/-}$ T cells in colon *lamina propria* from OVA-tolerized mice exposed to *fg*-SiO_2 through food pellets or oral gavage. At day 60, the frequency of $CD3^+$ $CD4^+$ T cells and of $CD3^+$ $CD4^+$ $CD25^+$ T cells in OVA-tolerized mice exposed to *fg*-SiO_2 was lower, regardless of the vehicle (Figure 4G,H; Figure S7), suggesting that *fg*-SiO_2 may limit local T cell expansion. In parallel, we found a lower gene expression of *foxp3* in the colon of OVA-tolerized mice exposed to *fg*-SiO_2 (Figure 4I), suggesting a reduction of $FOXP3^+$ Treg cells producing IL-10. Mice given *fg*-SiO_2 through food pellets showed no significant difference in $CD45^+$ $CD11b^+$ $CD103^+$ cell frequency, while this subset of cells was decreased in OVA-tolerized mice exposed to *fg*-SiO_2 through gastric gavage (Figure 4J; Figure S8).

Gluten Immunopathology in NOD/DQ8 Mice Exposed to Food-Grade SiO_2 and Challenged with Gluten

To explore the effect of *fg*-SiO_2 on gluten immunopathology, we used nonobese diabetic (NOD) mice expressing the DQ8 celiac disease susceptibility gene (NOD/DQ8). NOD/DQ8 mice were exposed daily to *fg*-SiO_2 by gavage at 10 mg/kg BW/d for 75 d and sensitized with gliadin, a well-characterized protein fraction in gluten, and cholera toxin from day 40 to day 61 before oral gluten challenges (Figure 5A). Anti-gliadin IgG2c and anti-transglutaminase 2 (tG2) IgG2c antibody levels were not accentuated in sensitized groups after a daily oral exposure to *fg*-SiO_2 (Figure 5B,C). However, a lower villus-to-crypt ratio and a

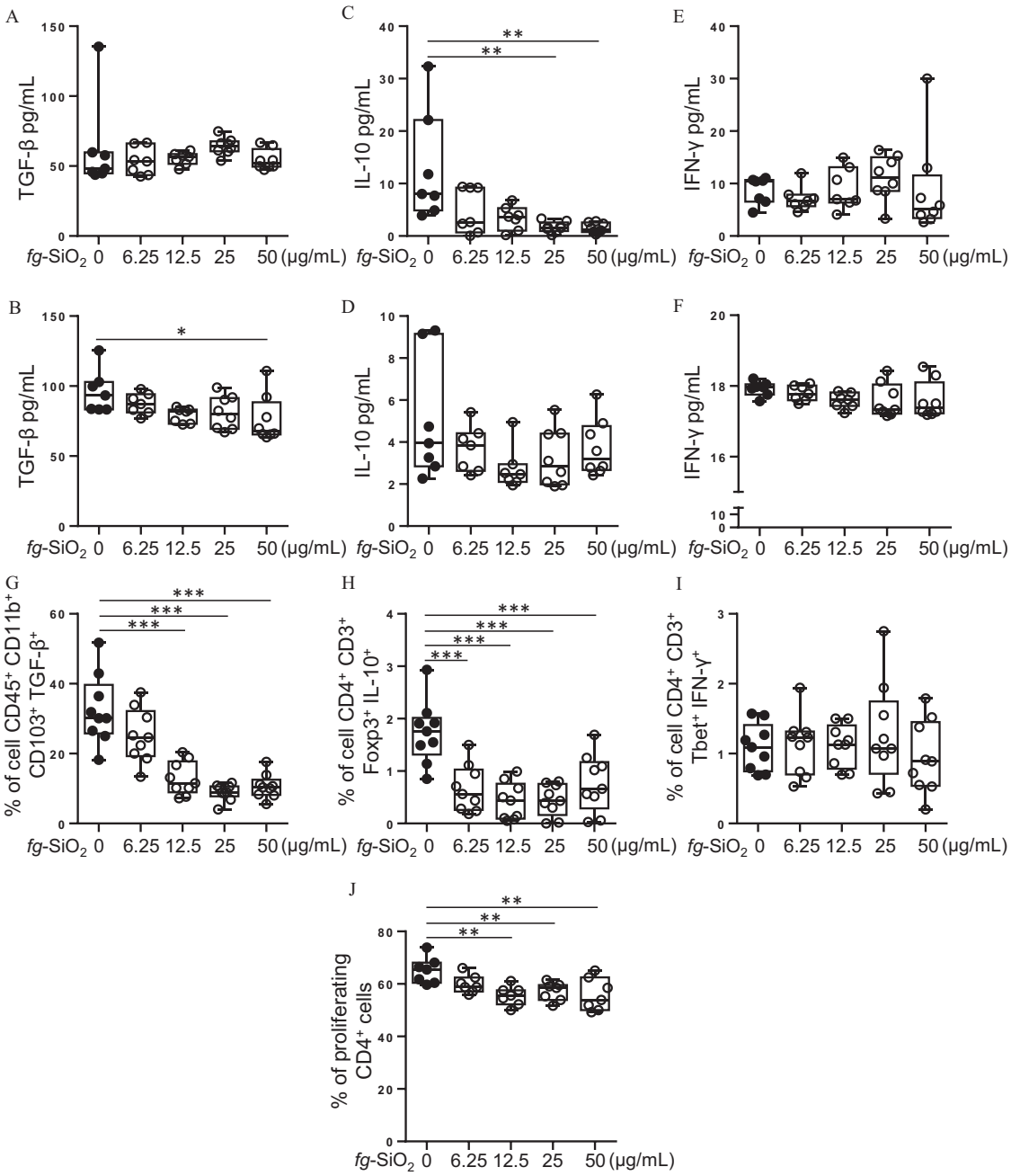

Figure 2. Evaluation of mesenteric lymph node (MLN) cell response after *ex vivo* exposure to food-grade SiO_2. (A–F) Cell suspension from MLN of untreated mice was stimulated in the presence of food-grade SiO_2 (*fg*-SiO_2) (0, 6.25, 12.5, 25, and 50 μg/mL) using an unspecific simulation with phorbol 12-myristate 13-acetate (PMA) and ionomycin (A,C,E) or an anti-CD3/anti-CD28 stimulation specific of T cells (B,D,F) ($n = 7$ per group for 0, 6.25, and 12.5 μg/mL and $n = 8$ per group for 25 and 50 μg/mL). Amount of TGF-β (A), IL-10 (C), and IFN-γ (E) secreted by MLN cells stimulated by PMA and ionomycin in the presence of *fg*-SiO_2 (0, 6.25, 12.5, 25, and 50 μg/mL). Secreted TGF-β (B), IL-10 (D) and IFN-γ (F) amounts by MLN cells stimulated by anti-CD3/anti-CD28 antibodies in the presence of *fg*-SiO_2 (0, 6.25, 12.5, 25, and 50 μg/mL). (G–I) Cell suspension from MLN of untreated mice ($n = 9$ per group) were exposed for 48 h to various concentrations of *fg*-SiO_2 (0, 6.25, 12.5, 25, and 50 μg/mL) before stimulation for 5 h with PMA and ionomycin. The frequency of $CD45^+$ $CD11b^+$ $CD103^+$ TGF-β^+ cells (i.e., antigen-presenting DC and macrophages) (G), regulatory T (Treg) cells IL-10^+ ($CD3^+$ $CD4^+$ $CD25^+$ $FoxP3^+$ IL-10^+) (H) and T helper 1 (Th1) cells IFN-γ^+ ($CD3^+$ $CD4^+$ $Tbet^+$IFN-γ^+) (I) was evaluated by flow cytometry. (J) Cell suspension from MLN of untreated mice was exposed for 3 d to concanavalin-A (a T-cell mitogen) in presence of *fg*-SiO_2 (0, 6.25, 12.5, 25, and 50 μg/mL) ($n = 7$ per group). Frequency of proliferative T cells was determined by measuring cell division with CellTrace Violet labeling and flow cytometry analysis. The data are expressed as median with interquartile range and whiskers extending from minimum to maximum ± SEM. $^*p < 0.05$; $^{**}p < 0.01$; $^{***}p < 0.001$ by one-way ANOVA and post hoc Tukey test (G–J) or Kruskal-Wallis test followed by a post hoc Dunn's test (A–F). Data behind graphs are reported in Table S4. Note: ANOVA, analysis of variance; DC, dendritic cells; IFN-γ, interferon gamma; IL-10, interleukin 10; SEM, standard error of the mean; TGF-β, transforming growth factor beta.

higher $CD3^+$ IEL count was observed after gluten challenge in mice exposed to *fg*-SiO_2 compared with those of mice not exposed to the food additive (Figure 5D–G). This was paralleled by higher duodenal gene expression of the pro-inflammatory cytokines *Ifnγ* and *Il17f* in NOD/DQ8 mice exposed to *fg*-SiO_2 (Figure 5H,I). Duodenal gene expression of *Il15*, a key cytokine in CeD, as well as that of *Il1β*, *Il10*, and *Tgfβ* were not different after *fg*-SiO_2 exposure (Figure 5J–M).

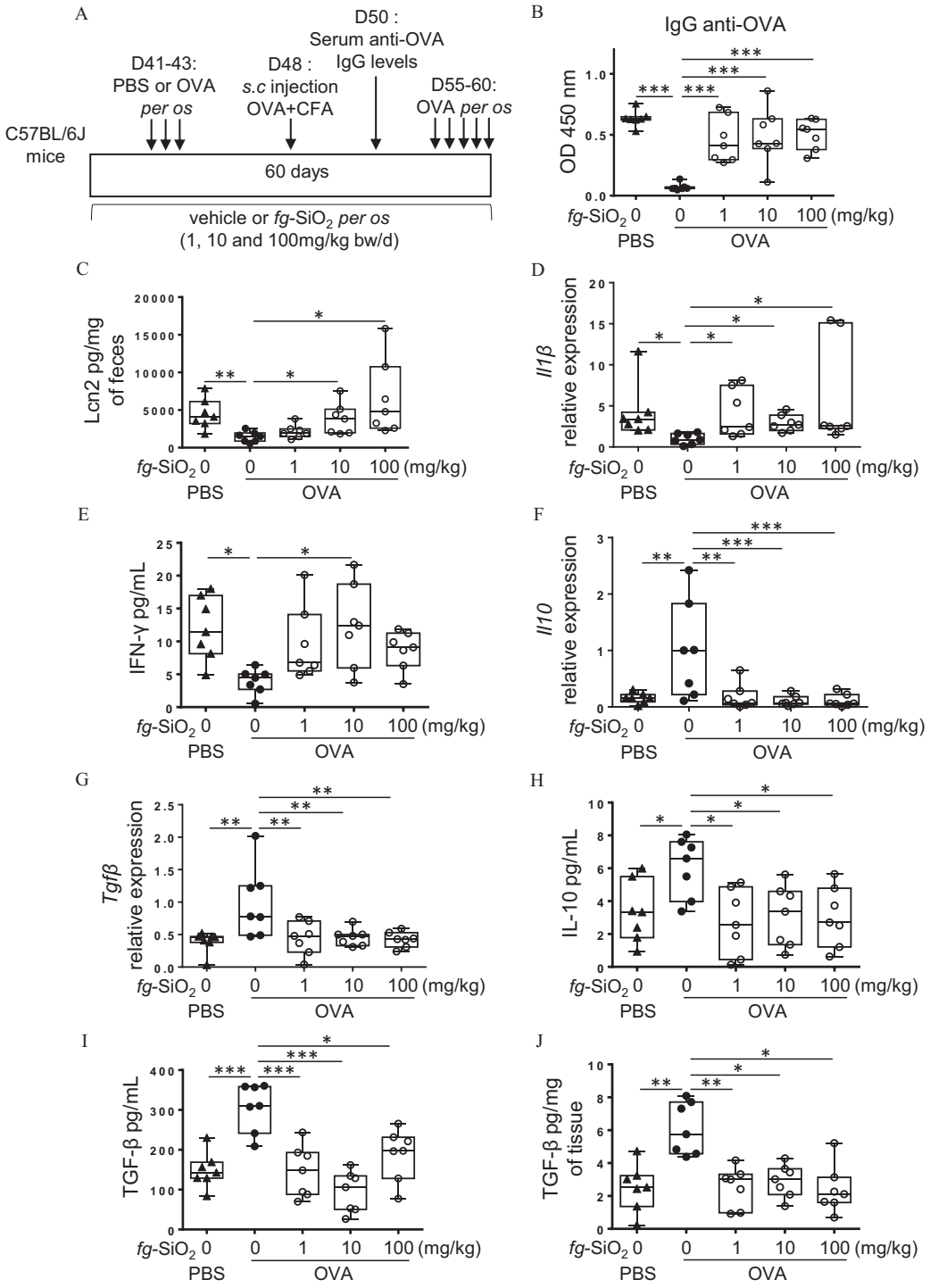

Figure 3. Evaluation of oral tolerance and gut immune response to ovalbumin in mice exposed 60 d to food-grade SiO_2. (A) The protocol of oral tolerance induction to ovalbumin (OVA) followed by a *de novo* challenge to OVA in C57BL/6J mice daily exposed to the vehicle (water) or to the food-grade SiO_2 (*fg*-SiO_2) (1, 10, or 100 mg/kg BW/d) through gavage. (B) OVA-specific IgG secretion in OVA-immunized (PBS) or OVA-tolerized mice exposed to a vehicle or *fg*-SiO_2 for 60 d ($n = 7$ mice per group). (C) Fecal lipocalin-2 (Lcn2) levels in OVA-immunized (PBS) or OVA-tolerized mice exposed to a vehicle or *fg*-SiO_2 for 60 d ($n = 7$ mice per group). (D) *Il*1β transcript expression in colon of OVA-immunized (PBS) or OVA-tolerized mice exposed to a vehicle or *fg*-SiO_2 for 60 d ($n = 7$ mice per group). (E) Amounts of IFN-γ secreted by mesenteric lymph node (MLN) cells from OVA-immunized (PBS) or OVA-tolerized mice exposed to a vehicle or *fg*-SiO_2 for 60 d ($n = 7$ mice per group). (F,G) *Il10* (F) and *Tgfβ* (G) transcript expression in colon of OVA-immunized (PBS) or OVA-tolerized mice exposed to a vehicle or *fg*-SiO_2 for 60 d ($n = 7$ mice per group). (H,I) Amounts of IL-10 (H) and TGF-β (I) secreted by mesenteric lymph node cells from OVA-immunized (PBS) or OVA-tolerized mice exposed to a vehicle or *fg*-SiO_2 for 60 d ($n = 7$ mice per group). Secreted TGF-β amounts by colon explants from OVA-immunized (PBS) or OVA-tolerized mice exposed to a vehicle or *fg*-SiO_2 for 60 d ($n = 7$ mice per group). The data are expressed as median with interquartile range and whiskers extending from minimum to maximum ± SEM. $^{*}p < 0.05$; $^{**}p < 0.01$; $^{***}p < 0.001$ by one-way ANOVA and post hoc Tukey test (E–J) or Kruskal-Wallis test followed by a post hoc Dunn's test (C,D). Data behind graphs are reported in Table S4. Note: ANOVA, analysis of variance; BW, body weight; CFA, complete Freund adjuvant; IgG, immunoglobulin G; IFN-γ, interferon gamma; IL-10, interleukin 10; OD, optical density; PBS, phosphate-buffered saline; SEM, standard error of the mean; TGF-β, transforming growth factor beta.

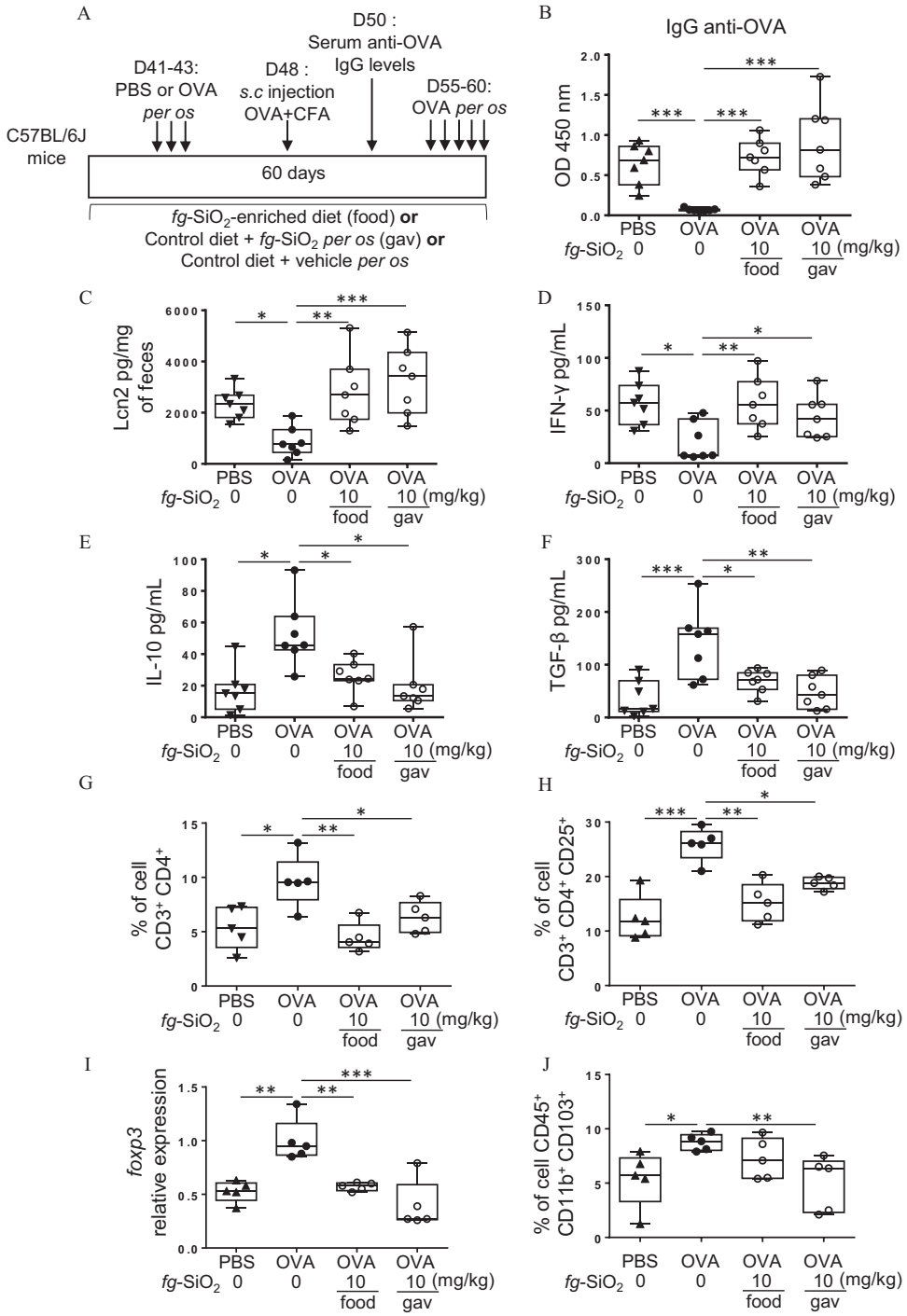

Figure 4. Evaluation of food matrix effects on food-grade SiO_2-mediated impairment of oral tolerance. (A) The protocol of oral tolerance induction to ovalbumin (OVA) followed by a *de novo* challenge to OVA in C57BL/6J mice daily treated for 60 d without (water gavage) or with food-grade SiO_2 (*fg*-SiO_2) (10 mg/kg BW/d) in water suspension [gastric gavage (gav)] or incorporated into food pellets (food). (B) OVA-specific IgG secretion in OVA-immunized (PBS) or OVA-tolerized mice exposed to a vehicle or *fg*-SiO_2 through gavage (gav) or food ($n=7$ mice per group). (C) Fecal lipocalin-2 (Lcn2) levels in OVA-immunized (PBS) or OVA-tolerized mice exposed to a vehicle or *fg*-SiO_2 through gavage (gav) or food ($n=7$ mice per group). (D–F) Amounts of IFN-γ (D), IL-10 (E), and TGF-β (F) secreted by mesenteric lymph node cells from OVA-immunized (PBS) or OVA-tolerized mice exposed to a vehicle or *fg*-SiO_2 through gavage (gav) or food ($n=7$ mice per group). (G,H) The average frequency of T cells ($CD3^+$ $CD4^+$) (G) and T cells $CD25^+$ ($CD3^+$ $CD4^+$ $CD25^+$) in colon *lamina propria* of OVA-immunized (PBS) or OVA-tolerized mice exposed to a vehicle or *fg*-SiO_2 through gavage (gav) or food ($n=5$ mice per group). *Foxp3* transcript expression in colon of OVA-immunized (PBS) or OVA-tolerized mice exposed to a vehicle or *fg*-SiO_2 through gavage (gav) or food ($n=5$ mice per group). (J) The average frequency of $CD45^+$ $CD11b^+$ $CD103^+$ cells (which fuses DC and macrophage subpopulations) in colon *lamina propria* of OVA-immunized (PBS) or OVA-tolerized mice exposed to a vehicle or *fg*-SiO_2 through gavage (gav) or food ($n=5$ mice per group). The data are expressed as median with interquartile range and whiskers extending from minimum to maximum ± SEM. $^{*}p<0.05$; $^{**}p<0.01$; $^{***}p<0.001$ by one-way ANOVA and post hoc Tukey test (B–I) or Kruskal-Wallis test followed by a post hoc Dunn's test (J). Data behind graphs are reported in Table S4. Note: ANOVA, analysis of variance; BW, body weight; CFA, complete Freund adjuvant; IgG, immunoglobulin G; IFN-γ, interferon gamma; IL-10, interleukin 10; OD, optical density; PBS, phosphate-buffered saline; SEM, standard error of the mean; TGF-β, transforming growth factor beta.

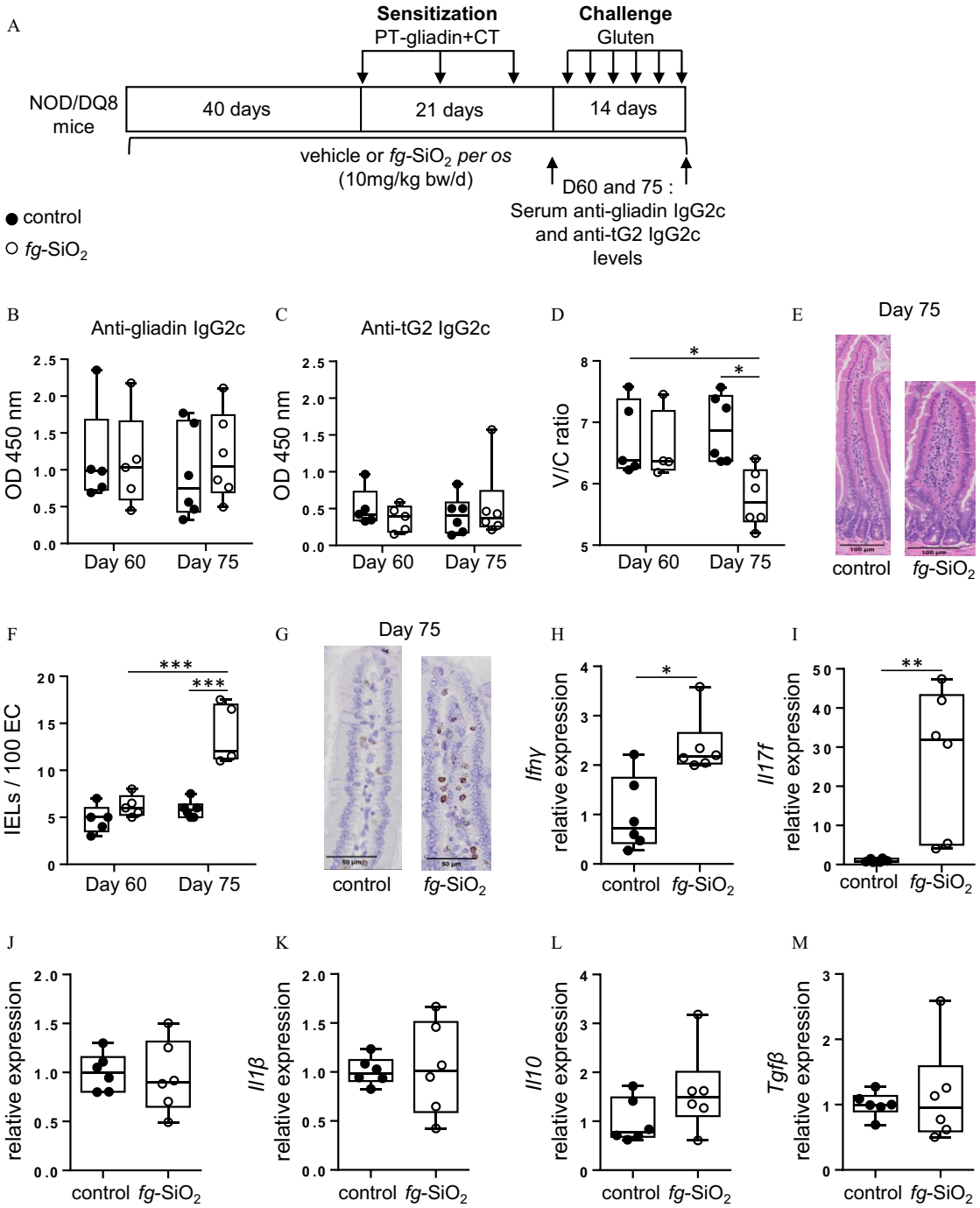

Figure 5. Evaluation of gluten immunopathology in NOD/DQ8 mice orally exposed to food-grade SiO_2. (A) Protocole for gliadin sensitization and challenge in NOD/DQ8 mice exposed to food-grade SiO_2 (*fg*-SiO_2) through gavage (10 mg/kg BW/d). (B,C) Levels of gliadin-specific IgG2c (B) and anti-transglutaminase 2 (tG2) IgG2c (C) antibodies in the serum of gliadin-sensitized (day 60, $n=5$ mice per group) and gluten-treated (day 75, $n=6$ mice per group) NOD/DQ8 mice orally exposed to *fg*-SiO_2 (white circle) or to the vehicle (black circle). (D) Villus-to-crypt ratios of gliadin-sensitized (day 60, $n=4/5$ mice per group) and gluten-treated (day 75, $n=6$ mice per group) NOD/DQ8 mice orally exposed to *fg*-SiO_2 (white circle) or to the vehicle (black circle). Due to the poor histological orientation of the small intestine during paraffin embedding, the evaluation of the villus-to-crypt ratios could not be performed on 1 gliadin-sensitized NOD/DQ8 mouse exposed to *fg*-SiO_2. (E) Representative hematoxylin and eosin-stained sections of proximal small intestine from gluten-treated NOD/DQ8 mice orally exposed to *fg*-SiO_2 or to the vehicle. (F) $CD3^+$ intraepithelial lymphocytes (IELs) (per 100 enterocytes) were counted in the proximal small intestine from gliadin-sensitized (day 60, $n=5$ mice per group) and gluten-treated (day 75, $n=5/6$ mice per group) NOD/DQ8 mice orally exposed to *fg*-SiO_2 (white circle) or to the vehicle (black circle). (G) Representative $CD3^+$ stained sections of proximal small intestine from gluten-treated NOD/DQ8 mice orally exposed to *fg*-SiO_2 or to the vehicle. (H–M) *Ifnγ* (H), *Il17f* (I), *Il15* (J), *Il1β* (K), *Il10* (L), and *Tgfβ* (M) transcript expression in proximal small intestine from gluten-treated NOD/DQ8 mice orally exposed to *fg*-SiO_2 or to the vehicle ($n=6$ mice per group). $^{*}p<0.05$; $^{**}p<0.01$; $^{***}p<0.001$ by one-way ANOVA and post hoc Tukey test (B–I) or Kruskal-Wallis test followed by a post hoc Dunn's test (J). The data are expressed as median with interquartile range and whiskers extending from minimum to maximum ± SEM. $^{*}p<0.05$; $^{**}p<0.01$; $^{***}p<0.001$ by one-way ANOVA and post hoc Tukey test (B,C,D,F) or by Student's two-tailed t test (H,J–L) or Mann-Whitney test (I,M). Data behind graphs are reported in Table S4. Note: ANOVA, analysis of variance; BW, body weight; CT, cholera toxin; IgG2c, immunoglobulin G2c; IFN-γ, interferon gamma; IL-10, interleukin 10; OD, optical density; PBS, phosphate-buffered saline; PT, pepsin-trypsin; SEM, standard error of the mean; TGF-β, transforming growth factor beta; tG2, tissue transglutaminase.

Discussion

Silicon dioxide, which is manufactured as a food ingredient and referred to as INS 551 (or E551 in the EU), is ingested daily by humans as nonsoluble nano-sized particles in the diet.[16] In humans, Si has been detected in liver, spleen, kidney, and intestine, without being able to determine whether the Si comes from the ingestion of foods containing natural (i.e., crystalline) Si (i.e., cereals, fruits, and vegetables) or from the absorption of the *fg*-SiO_2 as a food additive and manufactured from synthetic amorphous silica (SAS).[33,34] *In vivo* studies in rodents have detected Si in numerous organs following oral administration of SiO_2-NP models, including liver, kidney, brain, blood, and intestine.[34–36] While some studies in rodents have not revealed major toxicological outcomes,[34,37–41] others have demonstrated SiO_2-NPs can be hepatotoxic.[34–36,42–45] Different SiO_2 doses and routes of administration as well as duration of treatment could contribute to the differences observed between *in vivo* studies. Altogether, both animal and human studies demonstrate that there is absorption and systemic distribution of SiO_2-NPs after ingestion. Once SiO_2-NPs breach the intestinal mucosa,[40] they can interact with immune cells and modulate their response in the gut-associated lymphoid tissue,[20] blood,[14,35] or organs known to store Si.[35] A recent *in vivo* study based on NP models showed that SiO_2-NPs translocate through the gut epithelium inducing low-grade intestinal inflammation characterized by an increased production of the pro-inflammatory cytokines IL-1β, IL-6, and TNF-α.[20] However, this study employed nonfood nano-models, which were administered for short periods, thus not mimicking the chronic exposure to specific foodborne SiO_2-NPs daily consumed by the general population. Moreover, whether a daily exposure to *fg*-SiO_2 can affect intestinal immune responses to known food antigens triggering food sensitivities was not evaluated. Our results support a state of low-grade intestinal inflammation after long-term exposure to *fg*-SiO_2 that could favor host vulnerability to food sensitivities. Indeed, mice subjected to a 60-d exposure to *fg*-SiO_2 at human dietary levels had higher fecal Lcn-2 and intestinal IFN-γ production, which was associated with lower intestinal secretion of the anti-inflammatory cytokines IL-10 and TGF-β. These *fg*-SiO_2-mediated immunological defects could partly be due to a direct interaction of SiO_2 particles with intestinal immune cells, inhibiting T cell proliferation as well as IL-10 and TGF-β secretion by Treg and $CD45^+$ $CD103^+$ $CD11b^+$ DC, respectively. Despite several studies highlighting the variety of immunotoxic effects of SiO_2-NP models on cell lines[17,46–48] and bone marrow-derived cells,[48,49] as well as on systemic[50–53] and pulmonary immune cells,[54,55] the potential effects of these particles on intestinal immune cells remain poorly documented. In accordance with our results, the proliferation of T cells from spleen of mice orally exposed to SiO_2-NPs (750 mg/kg BW/day) for 14 d was significantly decreased compared to control.[53] Exposure of blood- or bone marrow-derived DC to SiO_2 particles promotes their activation and their production of pro-inflammatory cytokines in contrast to the herein reported effects on intestinal immune cells.[48–51] Overall, these results suggest that the immunological effects of SiO_2 particles differ according to the systemic or intestinal compartment of immune cells, with only the latter recognized as the induction site for OT establishment.[56,57]

As IL-10 and TGF-β are key cytokines involved in the establishment of OT,[56,57] we hypothesized that oral chronic exposure to *fg*-SiO_2 could interfere with this mechanism. Indeed, a previous study showed abrogation of OT induction to OVA in mice acutely exposed to nonfood SiO_2-NPs through gastric gavage for 5 d. However, doses higher than the mean level of adult human exposure were employed.[14] Nevertheless, splenocytes from OVA-tolerized mice exposed to nonfood SiO_2-NPs exhibited greater proliferation and secretion of IFN-γ (Th1), IL-17 (Th17), IL-4, and IL-5 (Th2) after an *ex vivo* restimulation with OVA.[14] This study suggested that SiO_2-NP models could abrogate OT by promoting Th1, Th2, and Th17 systemic immune responses.[14] However, the establishment of OT occurs at the intestinal level,[56,57] and the impact of chronic oral exposure to *fg*-SiO_2 on intestinal immune cells involved in OT induction remains unknown. We herein demonstrate that OVA-tolerized mice exposed to *fg*-SiO_2 through gastric gavage showed an impairment of OT induction. After *de novo* challenge with OVA, these mice exhibited higher fecal Lcn-2 and intestinal IFN-γ production, in parallel with lower intestinal IL-10 and TGF-β levels, demonstrating the development of low-grade inflammation in the gut mucosa. These effects were also observed when food-grade SiO_2 powder were mixed in food pellets given to mice, suggesting that chronic exposure to *fg*-SiO_2 at human dietary levels can impair OT to dietary antigens whatever the vehicle for feeding (i.e., in a solid or liquid matrix) by promoting gut inflammation.

Oral tolerance induction is mediated by the interaction of diverse intestinal immune cells, including $CD103^+$ DC, which produce TGF-β and present antigen to naive T-cells inducing their differentiation into $CD3^+$ $CD4^+$ $CD25^+$ Treg producing IL-10 or $CD3^+$ $CD4^+$ $CD25^-$ Tr1 cell secreting the immunoregulatory cytokines IL-10 and TGF-β.[56,57] In colon *lamina propria* of OVA-tolerized mice exposed to *fg*-SiO_2 through gastric gavage or food pellets, we found a lower proportion of $CD3^+$ $CD4^+$ $CD25^{+/-}$ T cells associated with a down-regulation of the expression of *foxp3*, used as a main identification marker for Treg cells. In addition, a lower frequency of $CD45^+$ $CD103^+$ $CD11b^+$ cells, i.e., which includes the gut DC in addition to macrophages,[58] was observed in colon *lamina propria* of OVA-tolerized mice exposed to *fg*-SiO_2 through gastric gavage compared with that of controls, while no significant difference in this subset of cells was found when exposure occurred through food pellets. The lack of significant effect on $CD45^+$ $CD103^+$ $CD11b^+$ cells in mice fed SiO_2 through food pellets could be due to the binding of food components on the NPs forming a protein/biomolecule corona, which could affect interaction with immune cells. Indeed, *in vitro* and/or *in vivo* studies demonstrated that food components influence the absorption and toxicity of inorganic NPs, such as zinc oxide (ZnO),[59,60] silver (Ag),[61,62] titanium dioxide (TiO_2),[63,64] and SiO_2.[65,66] In addition, amorphous silica NPs enhanced exogenous antigen entry and cross-presentation *in vitro* in murine DC, and this effect was suppressed after the modification of the NPs with either surface amine groups or carboxyl groups.[67] Together these results suggest that chronic *fg*-SiO_2 exposure at levels mimicking human chronic consumption blocks OT induction. This may result from an intestinal decrease of T cell proportion as well as of IL-10 and TGF-β production by Treg and $CD45^+$ $CD103^+$ $CD11b^+$ cells, which promotes a low-grade inflammatory environment in the gut mucosa. While the mechanism for impaired suppressive T cells in mice exposed to *fg*-SiO_2 remains unclear, it may be partly due to the observed decreased abundance of $CD45^+$ $CD103^+$ $CD11b^+$ cells (including antigen-presenting DC and macrophages), leading to a subsequent decrease in OVA presentation to naive T-cells. The underlying mechanisms by which *fg*-SiO_2 exposure hinders T cell proliferation and modulates cytokine production by immune cells supporting OT induction will be addressed in subsequent study. Overall, the results support breakdown of OT by chronic *fg*-SiO_2 administration, but its role in food sensitivity with autoimmune basis remains to be determined.

A previous study reported increased expression of *Ifnγ*, *Il15*, and *Il8* in biopsies from patients with CeD co-cultured with nonfood gold (Au)- or Ag- or TiO_2-NP and pepsin-trypsin gliadin.[68] However, the study did not assess SiO_2-NP and was based on acute exposure of biopsies, and no information on modulation of

immunopathology was reported. Using mice expressing the celiac risk gene HLA-DQ8, we performed daily oral administration of *fg*-SiO_2 for 75 d to investigate its effect on gluten-induced immunopathology. Gluten immunization of NOD/DQ8 results in intraepithelial lymphocytosis, reduced villus-to-crypt ratios, increased *Il15* expression, and mucosal barrier dysfunction.[29–31] We found that NOD/DQ8 mice given *fg*-SiO_2 showed greater reductions in villous to crypt ratios and higher $CD3^+$ IEL counts. In addition, chronic *fg*-SiO_2 treatment was found to be associated with higher duodenal expression of the pro-inflammatory cytokines *Ifnγ* and *Il17f* compared with sensitized mice that were not exposed to the food additive. These results demonstrate that chronic exposure to the food ingredient *fg*-SiO_2 exacerbates immunopathology in this model. This is noteworthy as IFN-γ is a key cytokine in CeD, which is associated with disease activity,[69–72] as its expression is higher not only compared with healthy controls[69–72] but with patients treated with a gluten-free diet.[69,72,73]

In summary, our study provides evidence that a chronic exposure to *fg*-SiO_2, a common food additive in the human diet, can disrupt intestinal immune homeostasis and initiate loss of OT and Th1 immunity to dietary antigens. The capacity for foodborne SiO_2 particles to trigger the loss of OT could be associated with its ability to decrease the intestinal abundance of specific T lymphocytes and $CD45^+$ $CD103^+$ $CD11b^+$ cells and their production of IL-10 and TGF-β, whose immunosuppressive functions pave the way for the physiological maintenance of OT. Moreover, our findings demonstrate worsened gluten immunopathology in NOD/DQ8 mice daily exposed to *fg*-SiO_2, raising the possibility that chronic exposure to this food additive could act as an environmental trigger in genetically susceptible people consuming gluten. This could be particularly relevant when combined with other environmental triggers such as reovirus infections[74] or bacterial opportunistic infections.[75–77] Our study provides a mechanistic basis for the role of chronic oral exposure to *fg*-SiO_2 as a food additive in food sensitivity and should encourage epidemiological investigation of this link in humans. Indeed, given the growing use of inorganic NPs in various industrial sectors (agriculture, automotive, medicine, food, cosmetics, textiles), and based on the current findings among other *in vivo* studies demonstrating a failure in the establishment of OT evoked by various inorganic particles,[14,78] it seems important to evaluate the role of the inorganic exposome in the increasing prevalence of food sensitivities.

Acknowledgments

B.L., N.M.B., E.F.V., and E.H. conceived and designed the study, analyzed the data, and wrote the manuscript. B.L. and N.M.B. designed and conducted all experiments, unless otherwise indicated; Y.M. performed and analyzed the RT-qPCR experiments; H.J.G. and M.W. designed and conducted the experiments with NOD/DQ8 mice and analyzed the histology and immunohistochemistry data; E.G., C.C., and Y.M. provided technical help for the *ex vivo* and *in vivo* experiments. B.L., N.M.B., E.F.V., and E.H. discussed the experiments and results.

We thank members of the animal facilities of EZOP (Toxalim) and McMaster University for the assistance in mouse care. We thank C. Richard, P.-A. Leitao, C. Ollivier, T. Parera, A. Guillard, and A. Pettes-Duler for technical help. The NOD/DQ8 mice were provided by J. A. Murray (Division of Gastroenterology and Hepatology, Department of Immunology, Mayo Clinic College of Medicine, Rochester, MN, USA).

This work was funded by the French National Research Agency (ANR-16-CE34-0011, PAIPITO grant) to B.L., N.M.B., and E.H. and a CIHR PJT grant-168840 to E.F.V. E.F.V. also holds a Tier 1 Canada Research Chair. M.W. was awarded the 2023 Dr. J.A. Campbell Young Investigator Award by Celiac Canada.

References

1. Ortolani C, Pastorello E. 2006. Food allergies and food intolerances. Best Pract Res Clin Gastroenterol 20(3):467–483, PMID: 16782524, https://doi.org/10.1016/j.bpg.2005.11.010.
2. Gargano D, Appanna R, Santonicola A, De Bartolomeis F, Stellato C, Cianferoni A, et al. 2021. Food allergy and intolerance: a narrative review on nutritional concerns. Nutrients 13(5):1638, PMID: 34068047, https://doi.org/10.3390/nu13051638.
3. Wambre E, Jeong D. 2018. Oral tolerance development and maintenance. Immunol Allergy Clin North Am 38(1):27–37, PMID: 29132672, https://doi.org/10.1016/j.iac.2017.09.003.
4. Nowak-Węgrzyn A, Katz Y, Mehr SS, Koletzko S. 2015. Non-IgE-mediated gastrointestinal food allergy. J Allergy Clin Immunol 135(5):1114–1124, PMID: 25956013, https://doi.org/10.1016/j.jaci.2015.03.025.
5. Meresse B, Ripoche J, Heyman M, Cerf-Bensussan N. 2009. Celiac disease: from oral tolerance to intestinal inflammation, autoimmunity and lymphomagenesis. Mucosal Immunol 2(1):8–23, PMID: 19079330, https://doi.org/10.1038/mi.2008.75.
6. Chinthrajah RS, Hernandez JD, Boyd SD, Galli SJ, Nadeau KC. 2016. Molecular and cellular mechanisms of food allergy and food tolerance. J Allergy Clin Immunol 137(4):984–997, PMID: 27059726, https://doi.org/10.1016/j.jaci.2016.02.004.
7. King JA, Jeong J, Underwood FE, Quan J, Panaccione N, Windsor JW, et al. 2020. Incidence of celiac disease is increasing over time: a systematic review and meta-analysis. Am J Gastroenterol 115(4):507–525, PMID: 32022718, https://doi.org/10.14309/ajg.0000000000000523.
8. Tang ML, Mullins RJ. 2017. Food allergy: is prevalence increasing? Intern Med J 47(3):256–261, PMID: 28260260, https://doi.org/10.1111/imj.13362.
9. Verdu EF, Caminero A. 2017. How infection can incite sensitivity to food. Science 356(6333):29–30, PMID: 28385972, https://doi.org/10.1126/science.aan1500.
10. Caminero A, Meisel M, Jabri B, Verdu EF. 2019. Mechanisms by which gut microorganisms influence food sensitivities. Nat Rev Gastroenterol Hepatol 16(1):7–18, PMID: 30214038, https://doi.org/10.1038/s41575-018-0064-z.
11. Issa M, Rivière G, Houdeau E, Adel-Patient K. 2022. Perinatal exposure to foodborne inorganic nanoparticles: a role in the susceptibility to food allergy? Front Allergy 3:1067281, PMID: 36545344, https://doi.org/10.3389/falgy.2022.1067281.
12. Lamas B, Martins Breyner N, Houdeau E. 2020. Impacts of foodborne inorganic nanoparticles on the gut microbiota-immune axis: potential consequences for host health. Part Fibre Toxicol 17(1):19, PMID: 32487227, https://doi.org/10.1186/s12989-020-00349-z.
13. Bettini S, Boutet-Robinet E, Cartier C, Coméra C, Gaultier E, Dupuy J, et al. 2017. Food-grade TiO2 impairs intestinal and systemic immune homeostasis, initiates preneoplastic lesions and promotes aberrant crypt development in the rat colon. Sci Rep 7:40373, PMID: 28106049, https://doi.org/10.1038/srep40373.
14. Toda T, Yoshino S. 2016. Amorphous nanosilica particles block induction of oral tolerance in mice. J Immunotoxicol 13(5):723–728, PMID: 27086695, https://doi.org/10.3109/1547691X.2016.1171266.
15. Lamas B, Chevalier L, Gaultier E, Cartier C, Weingarten L, Blanc X, et al. 2023. The food additive titanium dioxide hinders intestinal production of TGF-β and IL-10 in mice, and long-term exposure in adults or from perinatal life blocks oral tolerance to ovalbumin. Food Chem Toxicol 179:113974, PMID: 37516336, https://doi.org/10.1016/j.fct.2023.113974.
16. EFSA ANS Panel. 2018. Re-evaluation of silicon dioxide (E 551) as food additive. EFSA 16(1):5070–5088, https://doi.org/10.2903/j.efsa.2018.5088.
17. Dussert F, Arthaud P-A, Arnal M-E, Dalzon B, Torres A, Douki T, et al. 2020. Toxicity to RAW264.7 macrophages of silica nanoparticles and the E551 food additive, in combination with genotoxic agents. Nanomaterials (Basel) 10(7):1418, PMID: 32708108, https://doi.org/10.3390/nano10071418.
18. De Temmerman PJJ, Van Doren E, Verleysen E, Van der Stede Y, Francisco MA, Mast J. 2012. Quantitative characterization of agglomerates and aggregates of pyrogenic and precipitated amorphous silica nanomaterials by transmission electron microscopy. J Nanobiotechnology 10:24, PMID: 22709926, https://doi.org/10.1186/1477-3155-10-24.
19. U.S. Food & Drug Administration (FDA). 2022. GRAS Notice No. 996. https://www.fda.gov/media/156547/download [accessed 17 February 2022].
20. Chen H, Zhao R, Wang B, Cai C, Zheng L, Wang H, et al. 2017. The effects of orally administered Ag, TiO2 and SiO2 nanoparticles on gut microbiota composition and colitis induction in mice. Nanoimpact 8:80–88, https://doi.org/10.1016/j.impact.2017.07.005.
21. Powell JJ, Ainley CC, Harvey RS, Mason IM, Kendall MD, Sankey EA, et al. 1996. Characterisation of inorganic microparticles in pigment cells of human gut associated lymphoid tissue. Gut 38(3):390–395, PMID: 8675092, https://doi.org/10.1136/gut.38.3.390.

22. Hummel TZ, Kindermann A, Stokkers PC, Benninga MA, ten Kate FJ. 2014. Exogenous pigment in Peyer patches of children suspected of having IBD. J Pediatr Gastroenterol Nutr 58(4):477–480, PMID: 24164906, https://doi.org/10.1097/MPG.0000000000000221.
23. Galipeau HJ, Verdu EF. 2022. The double-edged sword of gut bacteria in celiac disease and implications for therapeutic potential. Mucosal Immunol 15(2):235–243, PMID: 35031683, https://doi.org/10.1038/s41385-021-00479-3.
24. Vignard J, Pettes-Duler A, Gaultier E, Cartier C, Weingarten L, Biesemeier A, et al. 2023. Food-grade titanium dioxide translocates across the buccal mucosa in pigs and induces genotoxicity in an in vitro model of human oral epithelium. Nanotoxicology 17(4):289–309, PMID: 37194738, https://doi.org/10.1080/17435390.2023.2210664.
25. Braniste V, Leveque M, Buisson-Brenac C, Bueno L, Fioramonti J, Houdeau E. 2009. Oestradiol decreases colonic permeability through oestrogen receptor beta-mediated up-regulation of occludin and junctional adhesion molecule-A in epithelial cells. J Physiol 587(pt 13):3317–3328, PMID: 19433574, https://doi.org/10.1113/jphysiol.2009.169300.
26. Menard S, Guzylack-Piriou L, Leveque M, Braniste V, Lencina C, Naturel M, et al. 2014. Food intolerance at adulthood after perinatal exposure to the endocrine disruptor bisphenol A. Faseb J 28(11):4893–4900, PMID: 25085925, https://doi.org/10.1096/fj.14-255380.
27. Lamas B, Richard ML, Leducq V, Pham H-P, Michel M-L, Da Costa G, et al. 2016. CARD9 impacts colitis by altering gut microbiota metabolism of tryptophan into aryl hydrocarbon receptor ligands. Nat Med 22(6):598–605, PMID: 27158904, https://doi.org/10.1038/nm.4102.
28. Lamas B, Michel M-L, Waldschmitt N, Pham H-P, Zacharioudaki V, Dupraz L, et al. 2018. Card9 mediates susceptibility to intestinal pathogens through microbiota modulation and control of bacterial virulence. Gut 67(10):1836–1844, PMID: 28790160, https://doi.org/10.1136/gutjnl-2017-314195.
29. Lamas B, Hernandez-Galan L, Galipeau HJ, Constante M, Clarizio A, Jury J, et al. 2020. Aryl hydrocarbon receptor ligand production by the gut microbiota is decreased in celiac disease leading to intestinal inflammation. Sci Transl Med 12(566):eaba0624, PMID: 33087499, https://doi.org/10.1126/scitranslmed.aba0624.
30. Galipeau HJ, McCarville JL, Huebener S, Litwin O, Meisel M, Jabri B, et al. 2015. Intestinal microbiota modulates gluten-induced immunopathology in humanized mice. Am J Pathol 185(11):2969–2982, PMID: 26456581, https://doi.org/10.1016/j.ajpath.2015.07.018.
31. Galipeau HJ, Rulli NE, Jury J, Huang X, Araya R, Murray JA, et al. 2011. Sensitization to gliadin induces moderate enteropathy and insulitis in nonobese diabetic-DQ8 mice. J Immunol 187(8):4338–4346, PMID: 21911598, https://doi.org/10.4049/jimmunol.1100854.
32. Chassaing B, Srinivasan G, Delgado MA, Young AN, Gewirtz AT, Vijay-Kumar M. 2012. Fecal lipocalin 2, a sensitive and broadly dynamic non-invasive biomarker for intestinal inflammation. PLoS One 7(9):e44328, PMID: 22957064, https://doi.org/10.1371/journal.pone.0044328.
33. Peters RJB, Oomen AG, van Bemmel G, van Vliet L, Undas AK, Munniks S, et al. 2020. Silicon dioxide and titanium dioxide particles found in human tissues. Nanotoxicology 14(3):420–432, PMID: 31994971, https://doi.org/10.1080/17435390.2020.1718232.
34. Brand W, van Kesteren P, Peters R, Oomen A. 2021. Issues currently complicating the risk assessment of synthetic amorphous silica (SAS) nanoparticles after oral exposure. Nanotoxicology 15:905–933, https://doi.org/10.1080/17435390.2021.1931724.
35. Tassinari R, Di Felice G, Butteroni C, Barletta B, Corinti S, Cubadda F, et al. 2020. Hazard identification of pyrogenic synthetic amorphous silica (NM-203) after sub-chronic oral exposure in rat: a multitarget approach. Food Chem Toxicol 137:111168, PMID: 32007467, https://doi.org/10.1016/j.fct.2020.111168.
36. McCracken C, Dutta P, Waldman J. 2016. Critical assessment of toxicological effects of ingested nanoparticles. Environ Sci: Nano 3(2):256–282, https://doi.org/10.1039/C5EN00242G.
37. Buesen R, Landsiedel R, Sauer UG, Wohlleben W, Groeters S, Strauss V, et al. 2014. Effects of SiO_2, ZrO_2, and $BaSO_4$ nanomaterials with or without surface functionalization upon 28-day oral exposure to rats. Arch Toxicol 88(10):1881–1906, PMID: 25164825, https://doi.org/10.1007/s00204-014-1337-0.
38. Cabellos J, Gimeno-Benito I, Catalán J, Lindberg HK, Vales G, Fernandez-Rosas E, et al. 2020. Short-term oral administration of non-porous and mesoporous silica did not induce local or systemic toxicity in mice. Nanotoxicology 14(10):1324–1341, PMID: 33108958, https://doi.org/10.1080/17435390.2020.1818325.
39. Kim M, Park J-H, Jeong H, Hong J, Choi WS, Lee B-H, et al. 2017. An evaluation of the in vivo safety of nonporous silica nanoparticles: ocular topical administration versus oral administration. Sci Rep 7(1):8238, PMID: 28811672, https://doi.org/10.1038/s41598-017-08843-9.
40. Yoshida T, Yoshioka Y, Takahashi H, Misato K, Mori T, Hirai T, et al. 2014. Intestinal absorption and biological effects of orally administered amorphous silica particles. Nanoscale Res Lett 9(1):532, PMID: 25288919, https://doi.org/10.1186/1556-276X-9-532.
41. Yun J-W, Kim S-H, You J-R, Kim WH, Jang J-J, Min S-K, et al. 2015. Comparative toxicity of silicon dioxide, silver and iron oxide nanoparticles after repeated oral administration to rats. J Appl Toxicol 35(6):681–693, PMID: 25752675, https://doi.org/10.1002/jat.3125.
42. van der Zande M, Vandebriel RJ, Groot MJ, Kramer E, Herrera Rivera ZE, Rasmussen K, et al. 2014. Sub-chronic toxicity study in rats orally exposed to nanostructured silica. Part Fibre Toxicol 11:8, PMID: 24507464, https://doi.org/10.1186/1743-8977-11-8.
43. Li J, He X, Yang Y, Li M, Xu C, Yu R. 2018. Risk assessment of silica nanoparticles on liver injury in metabolic syndrome mice induced by fructose. Sci Total Environ 628–629:366–374, PMID: 29448021, https://doi.org/10.1016/j.scitotenv.2018.02.047.
44. Hu H, Fan X, Guo Q, Wei X, Yang D, Zhang B, et al. 2019. Silicon dioxide nanoparticles induce insulin resistance through endoplasmic reticulum stress and generation of reactive oxygen species. Part Fibre Toxicol 16(1):41, PMID: 31699096, https://doi.org/10.1186/s12989-019-0327-z.
45. Boudard D, Aureli F, Laurent B, Sturm N, Raggi A, Antier E, et al. 2019. Chronic oral exposure to synthetic amorphous silica (NM-200) results in renal and liver lesions in mice. Kidney Int Rep 4(10):1463–1471, PMID: 31701056, https://doi.org/10.1016/j.ekir.2019.06.007.
46. Lucarelli M, Gatti AM, Savarino G, Quattroni P, Martinelli L, Monari E, et al. 2004. Innate defence functions of macrophages can be biased by nano-sized ceramic and metallic particles. Eur Cytokine Netw 15(4):339–346, PMID: 15627643.
47. Yang H, Wu QY, Lao CS, Li MY, Gao Y, Zheng Y, et al. 2016. Cytotoxicity and DNA damage in mouse macrophages exposed to silica nanoparticles. Genet Mol Res 15(3):15039005, PMID: 27706671, https://doi.org/10.4238/gmr.15039005.
48. Kang K, Lim JS. 2012. Induction of functional changes of dendritic cells by silica nanoparticles. Immune Netw 12(3):104–112, PMID: 22916046, https://doi.org/10.4110/in.2012.12.3.104.
49. Winter M, Beer HDD, Hornung V, Krämer U, Schins RP, Förster I. 2011. Activation of the inflammasome by amorphous silica and TiO2 nanoparticles in murine dendritic cells. Nanotoxicology 5(3):326–340, PMID: 20846021, https://doi.org/10.3109/17435390.2010.506957.
50. Guillet É, Brun É, Ferard C, Hardonnière K, Nabhan M, Legrand F-X, et al. 2023. Human dendritic cell maturation induced by amorphous silica nanoparticles is Syk-dependent and triggered by lipid raft aggregation. Part Fibre Toxicol 20(1):12, PMID: 37076877, https://doi.org/10.1186/s12989-023-00527-9.
51. Feray A, Guillet É, Szely N, Hullo M, Legrand F-X, Brun E, et al. 2021. Synthetic amorphous silica nanoparticles promote human dendritic cell maturation and CD4+ T-lymphocyte activation. Toxicol Sci 185(1):105–116, PMID: 34633463, https://doi.org/10.1093/toxsci/kfab120.
52. Tavares AM, Louro H, Antunes S, Quarré S, Simar S, De Temmerman P-J, et al. 2014. Genotoxicity evaluation of nanosized titanium dioxide, synthetic amorphous silica and multi-walled carbon nanotubes in human lymphocytes. Toxicol in Vitro 28(1):60–69, PMID: 23811260, https://doi.org/10.1016/j.tiv.2013.06.009.
53. Kim J-H, Kim C-S, Ignacio RMC, Kim D-H, Sajo MEJ, Maeng EH, et al. 2014. Immunotoxicity of silicon dioxide nanoparticles with different sizes and electrostatic charge. Int J Nanomedicine 9(Suppl 2):183–193, PMID: 25565836, https://doi.org/10.2147/IJN.S57934.
54. Beamer G, Seaver B, Jessop F, Shepherd D, Beamer C. 2016. Acute exposure to crystalline silica reduces macrophage activation in response to bacterial lipoproteins. Front Immunol 7:49, PMID: 26913035, https://doi.org/10.3389/fimmu.2016.00049.
55. Peeters PM, Eurlings IMJ, Perkins TN, Wouters EF, Schins RPF, Borm PJA, et al. 2014. Silica-induced NLRP3 inflammasome activation in vitro and in rat lungs. Part Fibre Toxicol 11(1):58, PMID: 25406505, https://doi.org/10.1186/s12989-014-0058-0.
56. Yu W, Freeland D, Nadeau K. 2016. Food allergy: immune mechanisms, diagnosis and immunotherapy. Nat Rev Immunol 16(12):751–765, PMID: 27795547, https://doi.org/10.1038/nri.2016.111.
57. Mowat A. 2003. Anatomical basis of tolerance and immunity to intestinal antigens. Nat Rev Immunol 3(4):331–341, PMID: 12669023, https://doi.org/10.1038/nri1057.
58. Bain CC, Montgomery J, Scott CL, Kel JM, Girard-Madoux MJH, Martens L, et al. 2017. TGFβR signalling controls CD103+CD11b+ dendritic cell development in the intestine. Nat Commun 8(1):620, PMID: 28931816, https://doi.org/10.1038/s41467-017-00658-6.
59. Jiang Q, Li X, Cheng S, Gu Y, Chen G, Shen Y, et al. 2016. Combined effects of low levels of palmitate on toxicity of ZnO nanoparticles to THP-1 macrophages. Environ Toxicol Pharmacol 48:103–109, PMID: 27770658, https://doi.org/10.1016/j.etap.2016.10.014.
60. Wang Y, Yuan L, Yao C, Ding L, Li C, Fang J, et al. 2014. A combined toxicity study of zinc oxide nanoparticles and vitamin C in food additives. Nanoscale 6(24):15333–15342, PMID: 25387158, https://doi.org/10.1039/c4nr05480f.

61. Böhmert L, Niemann B, Lichtenstein D, Juling S, Lampen A. 2015. Molecular mechanism of silver nanoparticles in human intestinal cells. Nanotoxicology 9(7):852–860, PMID: 25997095, https://doi.org/10.3109/17435390.2014.980760.
62. Lichtenstein D, Ebmeyer J, Knappe P, Juling S, Böhmert L, Selve S, et al. 2015. Impact of food components during in vitro digestion of silver nanoparticles on cellular uptake and cytotoxicity in intestinal cells. Biol Chem 396(11):1255–1264, PMID: 26040006, https://doi.org/10.1515/hsz-2015-0145.
63. Cao X, Zhang T, DeLoid GM, Gaffrey MJ, Weitz KK, Thrall BD, et al. 2020. Evaluation of the cytotoxic and cellular proteome impacts of food-grade TiO_2 (E171) using simulated gastrointestinal digestions and a tri-culture small intestinal epithelial model. NanoImpact 17:10, PMID: 32133427, https://doi.org/10.1016/j.impact.2019.100202.
64. Li Y, Jiang K, Cao H, Yuan M, Xu F. 2021. Influences of a standardized food matrix and gastrointestinal fluids on the physicochemical properties of titanium dioxide nanoparticles. RSC Adv 11(19):11568–11582, PMID: 35423614, https://doi.org/10.1039/d0ra09706c.
65. Go MRR, Bae SHH, Kim HJJ, Yu J, Choi SJJ. 2017. Interactions between food additive silica nanoparticles and food matrices. Front Microbiol 8:1013, PMID: 28638373, https://doi.org/10.3389/fmicb.2017.01013.
66. Lee J-A, Kim M-K, Song JH, Jo M-R, Yu J, Kim K-M, et al. 2017. Biokinetics of food additive silica nanoparticles and their interactions with food components. Colloids Surf B Biointerfaces 150:384–392, PMID: 27842933, https://doi.org/10.1016/j.colsurfb.2016.11.001.
67. Hirai T, Yoshioka Y, Takahashi H, Ichihashi K-I, Yoshida T, Tochigi S, et al. 2012. Amorphous silica nanoparticles enhance cross-presentation in murine dendritic cells. Biochem Biophys Res Commun 427(3):553–556, PMID: 23022188, https://doi.org/10.1016/j.bbrc.2012.09.095.
68. Mancuso C, Re F, Rivolta I, Elli L, Gnodi E, Beaulieu J-F, et al. 2021. Dietary nanoparticles interact with gluten peptides and alter the intestinal homeostasis increasing the risk of celiac disease. Int J Mol Sci 22(11):6102, PMID: 34198897, https://doi.org/10.3390/ijms22116102.
69. Przemioslo RT, Lundin KE, Sollid LM, Nelufer J, Ciclitira PJ. 1995. Histological changes in small bowel mucosa induced by gliadin sensitive T lymphocytes can be blocked by anti-interferon gamma antibody. Gut 36(6):874–879, PMID: 7615276, https://doi.org/10.1136/gut.36.6.874.
70. Nilsen EM, Jahnsen FL, Lundin KE, Johansen FE, Fausa O, Sollid LM, et al. 1998. Gluten induces an intestinal cytokine response strongly dominated by interferon gamma in patients with celiac disease. Gastroenterology 115(3):551–563, PMID: 9721152, https://doi.org/10.1016/s0016-5085(98)70134-9.
71. Kontakou M, Sturgess RP, Przemioslo RT, Limb GA, Nelufer JM, Ciclitira PJ. 1994. Detection of interferon gamma mRNA in the mucosa of patients with coeliac disease by in situ hybridisation. Gut 35(8):1037–1041, PMID: 7926902, https://doi.org/10.1136/gut.35.8.1037.
72. Wapenaar MC, van Belzen MJ, Fransen JH, Sarasqueta AF, Houwen RHJ, Meijer JWR, et al. 2004. The interferon gamma gene in celiac disease: augmented expression correlates with tissue damage but no evidence for genetic susceptibility. J Autoimmun 23(2):183–190, PMID: 15324937, https://doi.org/10.1016/j.jaut.2004.05.004.
73. Forsberg G, Hernell O, Melgar S, Israelsson A, Hammarström S, Hammarström M. 2002. Paradoxical coexpression of proinflammatory and down-regulatory cytokines in intestinal T cells in childhood celiac disease. Gastroenterology 123(3):667–678, PMID: 12198691, https://doi.org/10.1053/gast.2002.35355.
74. Bouziat R, Hinterleitner R, Brown JJ, Stencel-Baerenwald JE, Ikizler M, Mayassi T, et al. 2017. Reovirus infection triggers inflammatory responses to dietary antigens and development of celiac disease. Science 356(6333):44–50, PMID: 28386004, https://doi.org/10.1126/science.aah5298.
75. Caminero A, Galipeau HJ, McCarville JL, Johnston CW, Bernier SP, Russell AK, et al. 2016. Duodenal bacteria from patients with celiac disease and healthy subjects distinctly affect gluten breakdown and immunogenicity. Gastroenterology 151(4):670–683, PMID: 27373514, https://doi.org/10.1053/j.gastro.2016.06.041.
76. Caminero A, McCarville JL, Galipeau HJ, Deraison C, Bernier SP, Constante M, et al. 2019. Duodenal bacterial proteolytic activity determines sensitivity to dietary antigen through protease-activated receptor-2. Nat Commun 10(1):1198, PMID: 30867416, https://doi.org/10.1038/s41467-019-09037-9.
77. D'Argenio V, Casaburi G, Precone V, Pagliuca C, Colicchio R, Sarnataro D, et al. 2016. Metagenomics reveals dysbiosis and a potentially pathogenic N. flavescens strain in duodenum of adult celiac patients. Am J Gastroenterol 111(6):879–890, PMID: 27045926, https://doi.org/10.1038/ajg.2016.95.
78. Xu Y, Tang H, Wang H, Liu Y. 2015. Blockade of oral tolerance to ovalbumin in mice by silver nanoparticles. Nanomedicine (Lond) 10(3):419–431, PMID: 25707976, https://doi.org/10.2217/nnm.14.111.